AN ANALYSIS OF A FAST CARRIER RECOVERY SYSTEM FOR TDMA

by

© Carl Francis Weaver, B.A.Sc.

A Thesis

Submitted to the School of Graduate Studies

in Partial Fulfilment of the Requirements

for the Degree

Master of Engineering

McMaster University

November 1981

AN ANALYSIS OF A FAST CARRIER RECOVERY SYSTEM FOR TDMA

MASTER OF ENGINEERING (1981)
(Electrical Engineering)

McMaster University
Hamilton, Ontario

TITLE: An Analysis of a Fast Carrier Recovery System for TDMA

AUTHOR: Carl Francis Weaver, B.A.Sc. (University of Waterloo)

SUPERVISOR: Dr. D. P. Taylor, Department of Electrical and Computer Engineering

NUMBER OF PAGES: xiii, 80

ABSTRACT

Phase-locked loops occasionally exhibit prolonged phase transients and are therefore not suitable for carrier recovery applications in time division multiple access (TDMA) systems. Instead, designers have, in several cases, used a single-tuned high Q filter in combination with an automatic frequency control. A non-linear differential equation model for such a system, called a "frequency locked loop" (FLL) is solved by computer to obtain the transient responses. The solutions obtained indicate that the FLL has fast and reliable carrier phase acquisition times compared to a phase-locked loop (PLL). Also, since the non-linear responses agree well with linear model responses, an equation based on the linear model is developed to determine worst-case acquisition time. It is shown that a limiter preceeding the single-tuned tank does not directly affect acquisition performance and will improve noise performance of the FLL. With a limiter, the FLL block diagram is equivalent to an FM feedback demodulator (FMFB) on which there is a large amount of existing literature. Using results from the literature, it is demonstrated how the FMFB will perform in the presence of Gaussian noise. Finally, a design procedure is recommended which takes into account the tradeoff between noise performance and acquisition/tracking ability and attempts to minimize the acquisition time for a given level of Gaussian noise.

ACKNOWLEDGEMENTS

I would like to thank my supervisor Dr. D. P. Taylor for his direction and encouragement in the research for this thesis. I would like to thank Miller Communication Systems Limited and several of their employees; namely, R. Bedford, R. G. Lyons and F. Vaughan, for experimental results which they provided to me and for several discussions which we have had. Also, I would like to thank two fellow graduate students; namely, G. R. McMillen, for some very helpful criticisms of critical parts of the research, and V. R. Kezys, for his "software packages", and Ms. L. Hunter, for assistance in organization and typing of my thesis.

From my previous life as an employee of Raytheon Canada Limited, I would like to thank all of the people who have given me inspiration then, and in my present research activities. Some of these people are: M. Earle, E. Fiskvatn, Dr. N. A. Liskov, A. Lodberg, T. Miskiewicz, R. E. Moutray, P. J. Tanzi and E. White.

TABLE OF CONTENTS

LIST OF FIGURES

GLOSSARY OF SYMBOLS

Except for Laplace transfer functions and impulse responses, time dependent variables are given in this glossary without the time dependence indicated, however, the time dependence is indicated in the text of the thesis. The same symbols may also be used in the thesis as Laplace transform variables in which case they would be written as functions of "s". For example, the symbol e_s which represents the error signal is a time variable as $e_s(t)$ or it could be used as the Laplace transform of the error signal as $e_s(s)$. The symbols used are in alphabetic order with English alphabet first and Greek alphabet second.

A	Peak amplitude of the carrier at the STT input when limiter is not used (volts)
B	Peak amplitude of carrier at the STT input when an ideal hard limiter is used (volts)
B_N	Closed loop noise bandwidth (Hertz)
b	Empirical factor required to compensate for non-linearity of error detector in predicting acquisition times for large frequency offsets
D	$D = \sqrt{1 - \delta^2}$
f_I	Input frequency offset to frequency tracking loop (Hertz)
e_f	Filtered error signal (volts)
e_{fs}	Steady-state filtered error signal (volts)
e_s	Difference frequency error signal (volts)
e_{ss}	Steady-state filtered error signal (volts)
$F(s)$	Laplace transfer function of loop low-pass filter
$h(t)$	Impulse response of the STT (Single-tuned tank)
$H(s)$	Laplace transfer function of the STT
$H_b(s)$	Baseband equivalent Laplace transfer function of the STT
K_a	Loop amplifier amplitude gain factor
K_d	Phase detector sensitivity (volt/radion)
K_o	VCO sensitivity (radian/s/volt)
K_{OL}	Open loop amplitude gain
K_V	Error signal gain: $K_V = K_{OL}/\tau$. (s^{-1})
N	Average number of "clicks" per second in limiter-discriminator frequency demodulator. (s^{-1})

N_o	Noise spectral density (watt/Hz)
n_s	Peak amplitude of narrow-band Gaussian noise in sine dimension (volt)
n_c	Peak amplitude of narrow-band Gaussian noise in cosine dimension (volt)
Q	Quality factor of STT
t_a	Time required for frequency tracking loop to obtain a suitable phase reference (s)
t_{aw}	Worst case value of t_a (s)
T_D	Time delay required to provide $\pi/2$ phase shift at angular frequency of ω_o (s)
v_o	STT input signal (volt)
v_i	STT input signal (volt)
v_c	STT capacitor voltage (volt)
v_p	Phase shifter output signal (volt)
v_e	Phase shifter intermediate signal (volt)
v_q	Phase detector input signal (volt)
v_{lo}	A low-pass filter output signal (volt)
v_{li}	A low-pass filter input signal (volt)
v_{ib}	Complex baseband STT input signal (volt)
v_{ob}	Complex baseband STT output signal (volt)
δ	Damping ratio of FLL closed loop response
θ_e	Phase of STT baseband input signal (rad)
θ_{es}	Steady-state phase of STT baseband input signal (rad)
θ_f	Phase of STT bandpass input signal (rad)

θ_v	Phase of VCO baseband output signal (rad)
θ_{vs}	Steady-state phase of VCO baseband output signal (rad)
θ_s	Phase difference between STT input and output signals (rad)
θ_{sm}	Maximum allowable phase difference θ_s for acceptable demodulation (rad)
θ_{sfm}	Maximum expected value of steady-state phase difference θ_s which is dependent on maximum expected frequency offset ω_{IM} (rad)
θ_r	Output phase of FLL with down and up conversion (rad)
θ_I	Input phase to FLL (rad)
θ_o	Output phase of FLL with down conversion only (rad)
$\overline{\theta}_{vn}^2$	Mean square VCO output phase jitter due to noise in loop (rad^2)
ρ	Carrier-to-noise ratio at FLL input
ρ_m	Minimum carrier-to-noise ratio at which FLL is intended to operate
τ	STT time constant (s)
τ_c	First-order loop time constant (s)
τ_f	Loop low-pass filter time constant (s)
τ_x	Matched filter approximate time constant (s)
$\phi(t)$	$\phi(t) = \omega_n D t - \tan^{-1} (\frac{D}{\delta})$ (rad)
ω_{co}	VCO bandpass output frequency (rad/s)
ω_e	STT input frequency tracking error (rad/s)
ω_{es}	Steady-state STT input frequency tracking error (rad/s)
ω_{em}	Value of ω_e which gives maximum steady-state error signal for frequency detector without a limiter (rad/s)
ω_d	Imaginary part of natural frequency of the STT (rad/s)
ω_f	STT input frequency (rad/s)
ω_3	STT 3dB bandwidth (rad/s)

ω_I	FLL input offset frequency (rad/s)
ω_{IF}	FLL input frequency (rad/s)
ω_{IM}	Maximum expected FLL input offset frequency (rad/s)
ω_L	Loop low-pass filter 3 dB bandwidth (rad/s)
ω_n	Natural frequency of the FLL closed-loop response (rad/s)
ω_o	Resonant frequency of STT (rad/s)

CHAPTER 1

INTRODUCTION

1.1 Burst Modems and TDMA

Time Division Multiple Access (TDMA) is a method of time sharing a communication channel among many users. TDMA is primarily used on satellite communication channels. In a satellite TDMA system, a single user transmits over the channel for a small fraction of the available time by sending information in periodic bursts. Practically all satellite systems use coherent demodulation and suppressed carrier modulation and it is necessary to recover a carrier reference from the modulation. With short burst lengths, the time for a carrier recovery circuit to obtain a suitable carrier can become a significant overhead on the utilization of the channel. For that reason, an important parameter of burst modems is the time required to acquire a suitable carrier reference, bit timing reference, and symbol timing reference. This time is often called acquisition time. The importance of short acquisition time for burst modems is the one major difference between burst modems and modems intended for continuous transmission.

1.2 Acquisition of Carrier Reference

Carrier phase is usually estimated for QAM* and PSK* digital modulations by one of three common methods. These are: Decision feedback

* Quadrature Amplitude Modulation (QAM), Phase Shift Keying (PSK)

or remodulation loops, nth power loops and Costas loops. Costas loops and power loops are theoretically the same and do not require bit decisions. Decision feedback requires the bit decisions to modulate the received modulated carrier in a sense opposite to the original modulation and thus to remove the modulation. Figure 1.1 shows a squaring loop and a decision feedback approach, implemented using phase lock loop (PLL) techniques.

Costas loops inherently contain a PLL while power loops and decision feedback loops do not necessarily require a PLL, but are normally designed using PLL's. The nth power loops can be separated into the cascade of an nth power device and a carrier filter. The decision feedback circuit can also be separated into a remodulation circuit and a carrier filter (Figure 1.1). As noted above, the filter is normally implemented with a PLL, however, for TDMA applications where fast acquisition of a carrier reference is a requirement, there is a significant problem with PLL tracking filters. This problem is known as hang up and manifests itself through occasional prolonged phase transients.

1.3 Hang Up in PLL Carrier Filters

"Hang up" in Phase Lock Loops (PLL) [10] is a condition arising when the initial phase error is at the reverse slope zero crossing of the periodic phase detector characteristic. The restoring force at this unstable null is small (in principle, zero) and noise can cause the loop to jitter about the null. Thus, hang up can cause long acquisition times. Since it is important to have fast carrier acquisition with high reliability, a conventional PLL is thus not very suitable for TDMA applic-

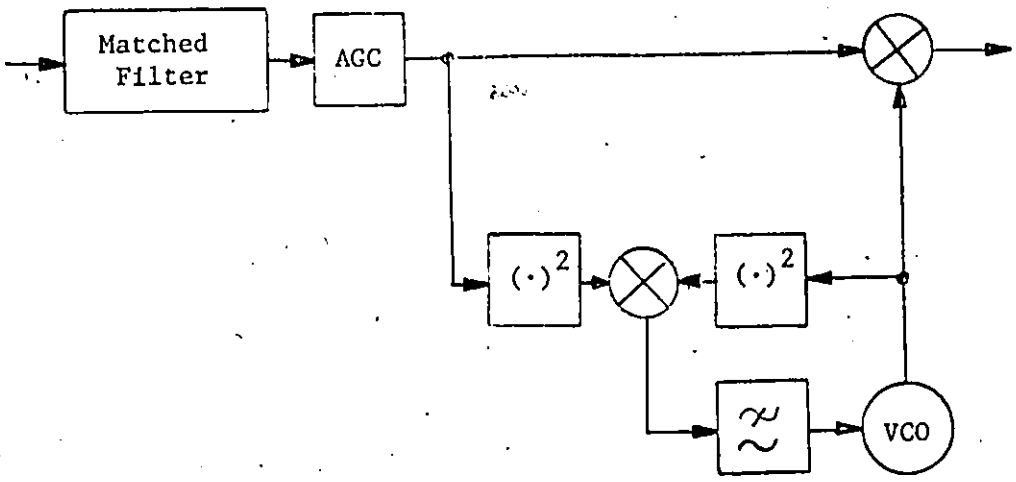

Figure 1.1 (a): Squaring Recovery Loop for a BPSK Receiver

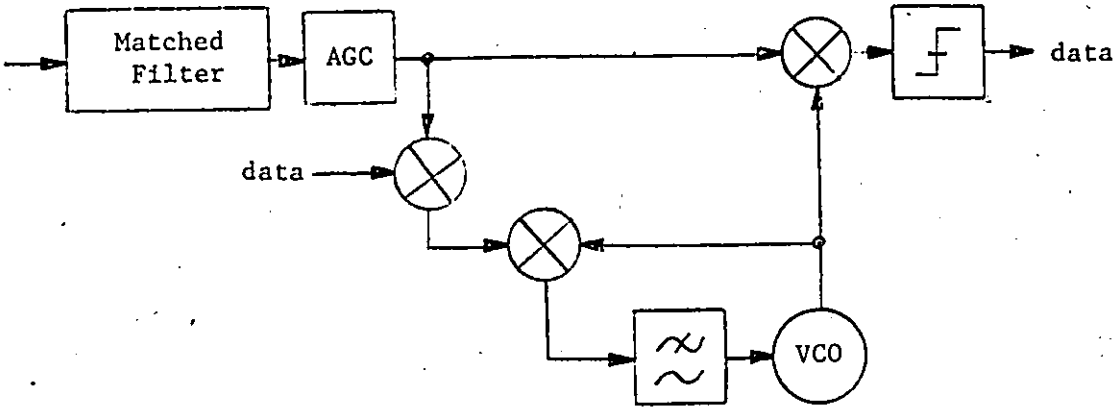

Figure 1.1 (b): Remodulation Recovery Loop for a BPSK Receiver

ations. Some designers [12] [13] have constructed phase detectors which were intended to remove the hang up problem. Others [1] [11] [14] [15] have used fixed single-tuned and multi-tuned filters with automatic frequency control (AFC) to serve as carrier filters.

1.4 An Alternate Carrier Filter

One alternative to a PLL is a high Q tuned filter centered at the carrier frequency. One problem with this idea is that the frequency drifting of the received carrier will cause phase shift of the recovered carrier relative to the modulated carrier, because of the large slope of phase versus frequency in a high Q filter. A high Q filter could be used, however, if AFC is used to minimize the frequency variation and resultant phase shift through the filter. An approach such as this is shown in Figure 1.2. This approach is also used in [1, 2, 3, 14, 15].

Referring to Figure 1.2, the high Q filter is designed with resonant frequency ω_o. A controlled reference oscillator at frequency ω_{co} is used to convert the carrier frequency ω_{IF} to a frequency $\omega_o + \omega_e$ and back again to frequency ω_{IF}. The VCO is adjusted to minimize the error frequency ω_e and thereby to minimize the variation in phase of the recovered carrier.

To minimize the frequency error, ω_e, an error signal proportional to ω_e is desired. Since any high Q filter has a phase response that varies with frequency, comparing the input and output of the high Q filter with a phase detector would give an error signal related to frequency. It is desired to have an error signal characteristic with only one zero

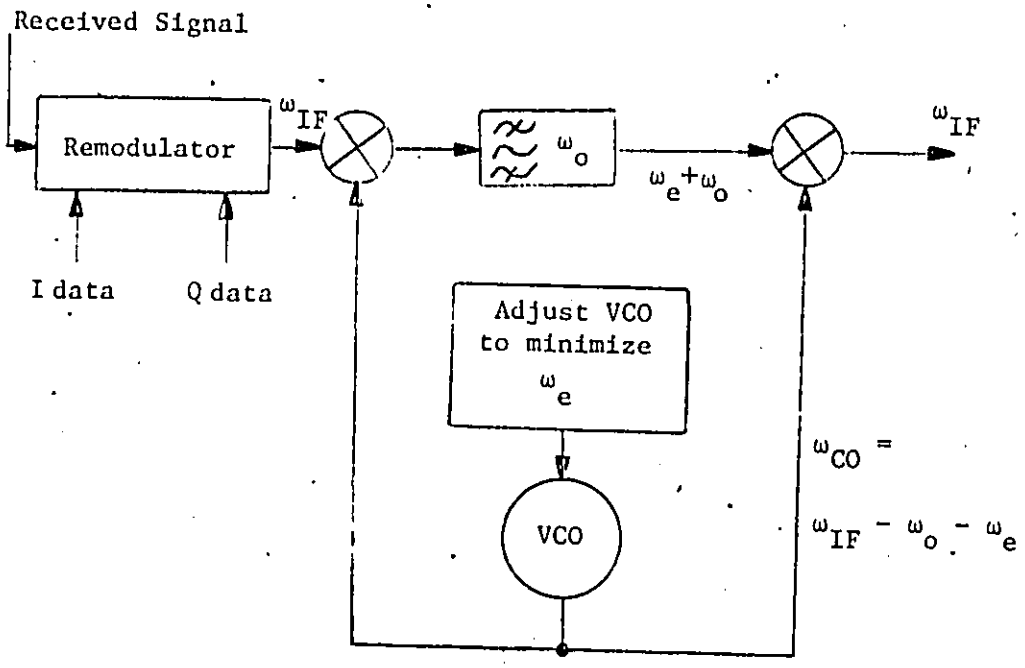

Figure 1.2: Alternate Approach to Carrier Filtering with Signal Frequencies Shown

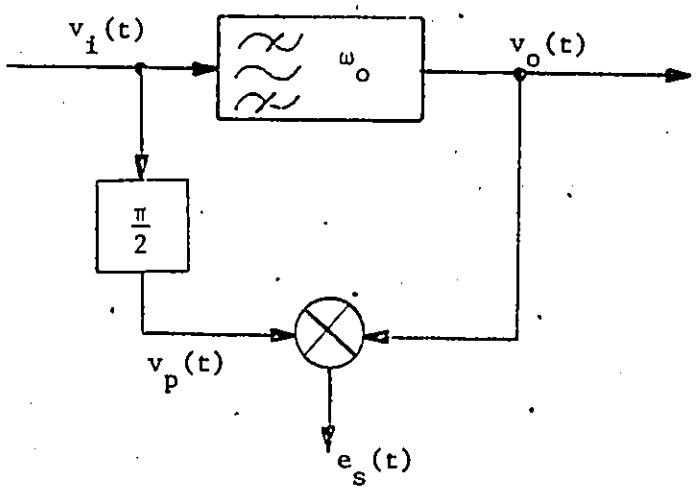

Figure 1.3: Frequency Error Detector

crossing occurring at a frequency of ω_o. Since a mixer type phase detector has zero crossings every 180^o of phase, then to have one zero crossing in the error signal characteristic means that the high Q filter cannot have more than 4 poles, or in other words, it must be a double-tuned tank (DTT) or single-tuned tank (STT). For this thesis only, a STT is considered. This proposed error signal detector is used in references [1, 2, 3, 14] and is shown in Figure 1.3. The 90^o phase shifter shown is necessary in order to place the zero crossing at ω_o since an STT has 0^o phase shift at ω_o. This is shown in an analysis of the error signal in Chapter 2.0.

For the remainder of this thesis, the circuit described here, (of Figure 1.2) for convenience, will be referred to as a frequency locked loop (FLL) because of its resemblance to a PLL. The only fundamental difference between the PLL and FLL lies in the use of a phase detector in the former, rather than a frequency detector.

1.5 Scope of Thesis

The purpose of this thesis is to gain a better understanding of the carrier acquisition performance and the noise performance of the FLL, and to develop appropriate analyses. In Chapter 2, the basic FLL operation is examined, the steady-state operation is investigated, and an attempt is made to develop a linear model under several restrictions. Finally, in Chapter 2, the critical loop parameters are identified and methods of measurement are given. In Chapter 3, several nonlinear differential equation models are developed for the FLL in order to obtain the transient responses of the loop by computer. Many transient resp-

onses are computed, which give much insight into loop operation. The linear model from Chapter 2 as well as measured results are compared to the differential equation model. In Chapter 4, the effects of noise are considered. The use of limiters is discussed and the equivalence of the FLL to an FM feedback (FMFB) demodulator is noted. Finally, in Chapter 4, frequency "clicks" associated with FM threshold are considered (analogous to cycle slips in PLL's) and the relation of the loop parameters to the probability of frequency "clicks" or threshold is discussed. Chapter 5 contains conclusions and recommendation for further work.

CHAPTER 2

FREQUENCY-LOCKED LOOP: BASIC OPERATION

2.1 Loop Models

Figures 2.1 and 2.2 show two principle applications of the frequency-locked loop (FLL) to coherent demodulation. The limiters in both figures are shown as dashed lines because either one or both of them may be used. The use of limiters in the FLL will be discussed further in Chapter 4. The FLL method of carrier filtering could be applied equally well to nth power loop recovery systems. In the above figures, remodulation has been used to remove the data modulation.

Since in the TDMA application under consideration [2] an all ones pattern is transmitted during the acquisition period, the remodulation circuit should have no effect, and except for the transient response of the channel, which includes the matched filter and automatic gain control (AGC), a sinusoidal signal is expected at the remodulator output in Figure 2.2.

In order to study loop behaviour, the models of Figures 2.3 and 2.4 may be used. The mixer used for frequency translation in Figure 2.2 may be considered as a summer with respect to the frequency variables as shown in Figure 2.3. The voltage controlled oscillator (VCO) frequency, $\omega_{co}(t)$, is subtracted from the input frequency, ω_{IN}, to get the single-tuned tank (STT) input frequency $\omega_f(t)$. These fre-

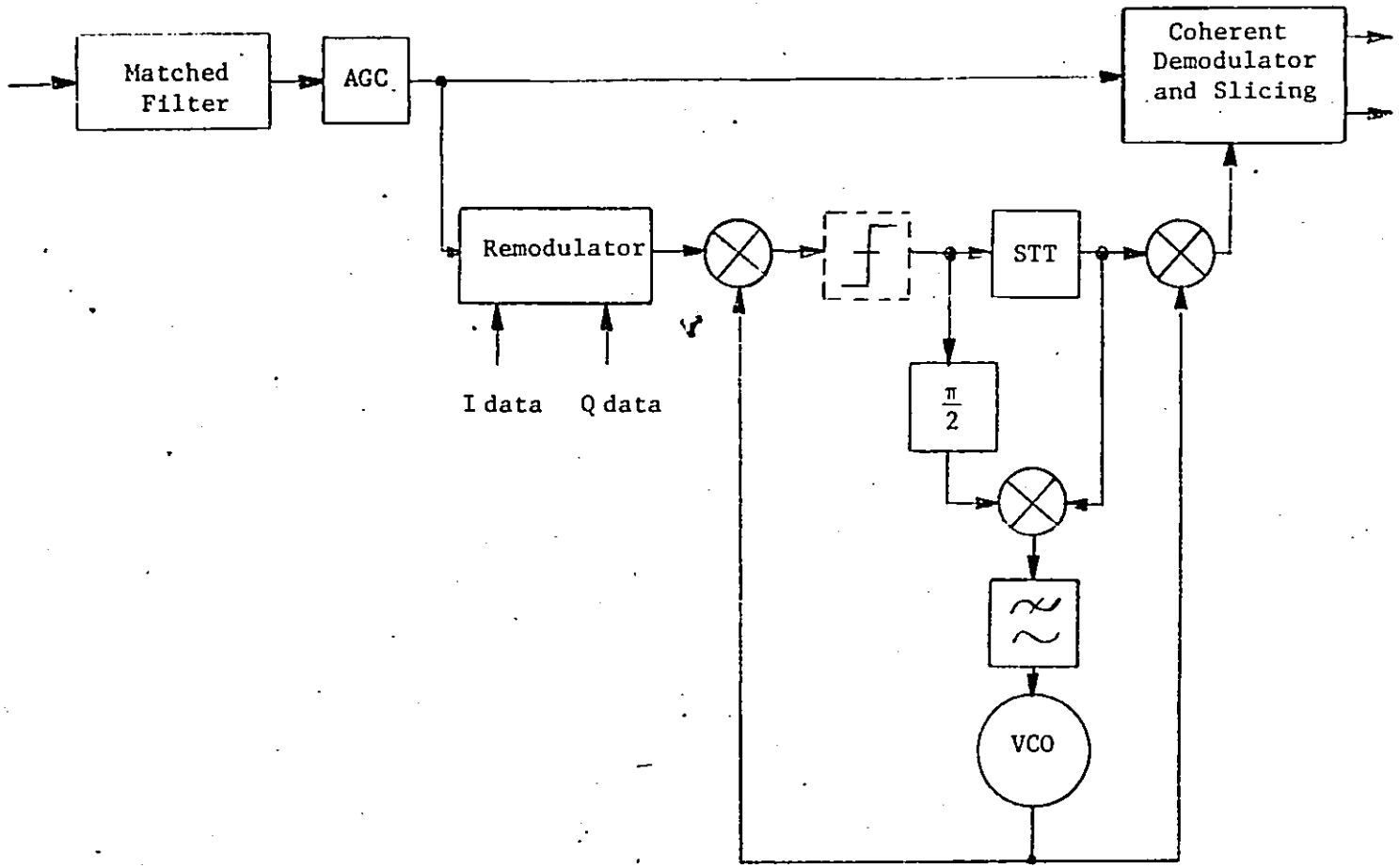

Figure 2.1: Application of Frequency Tracking Loop with Down and Up Conversion

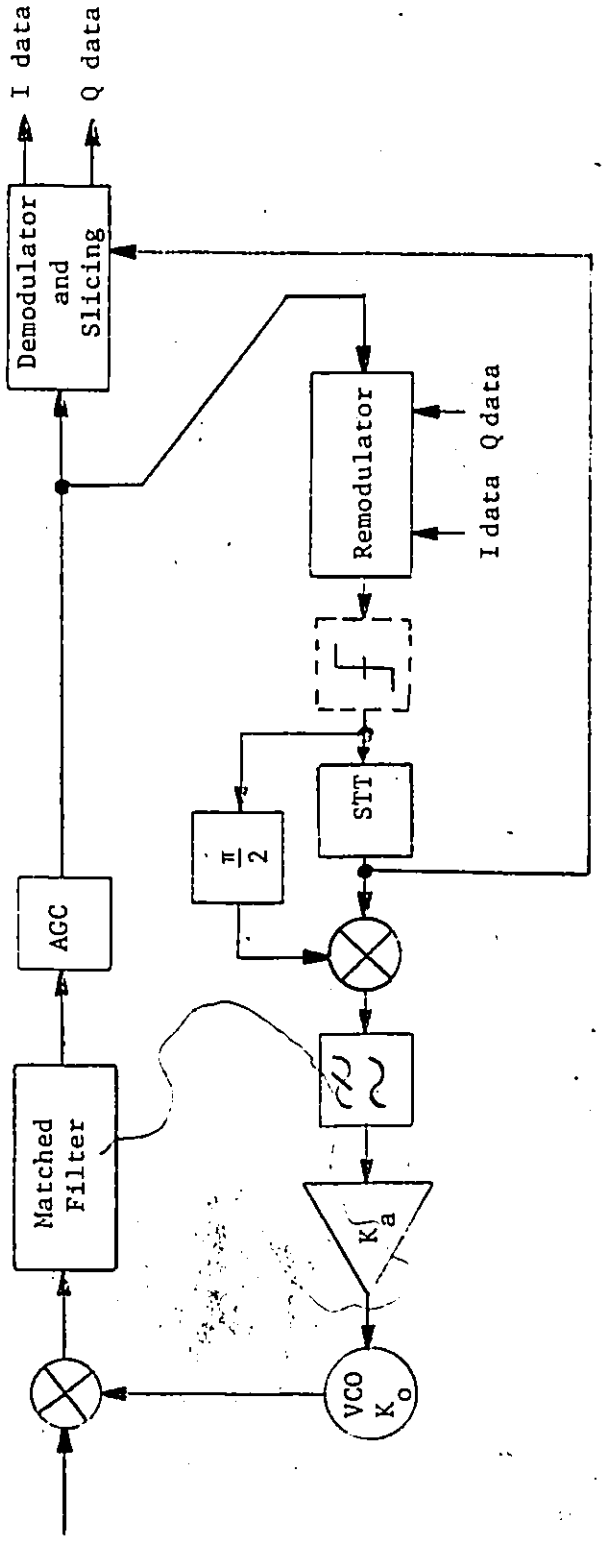

Figure 2.2: Application of Frequency Tracking Loop with Down Conversion only

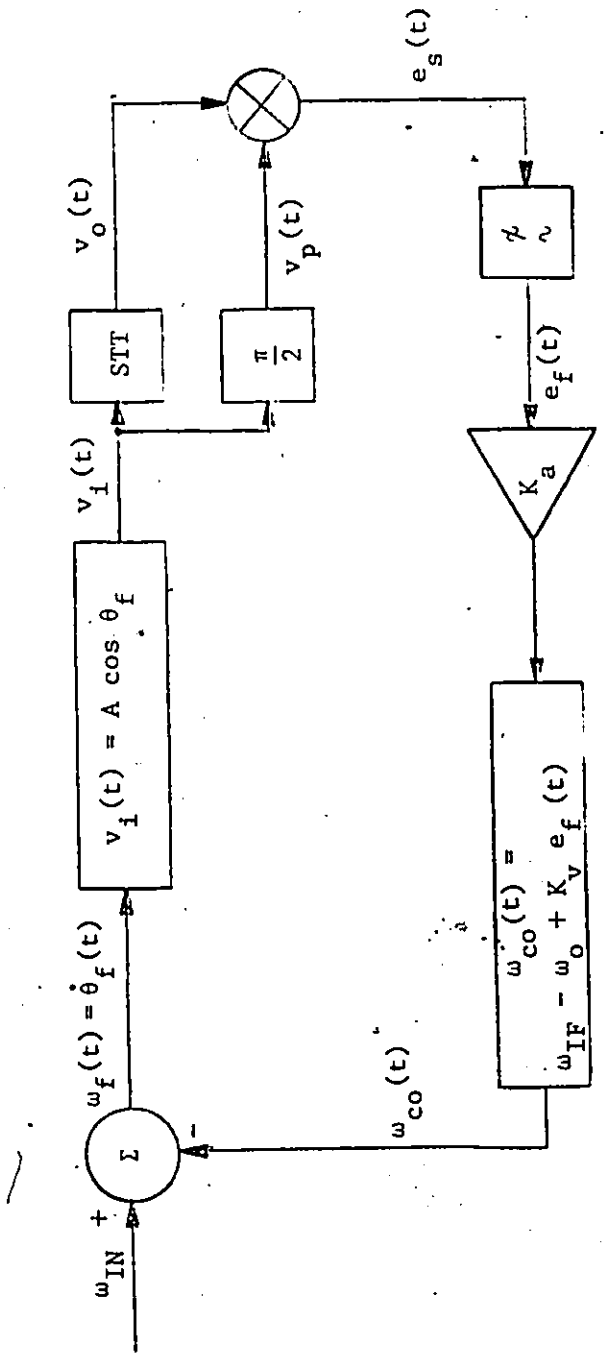

Figure 2.3: Loop Model

quencies are related as:

$$\omega_{IN} = \omega_{IF} + \omega_I \tag{2.1.1}$$

$$\omega_{co}(t) = \omega_{IF} - \omega_o + \omega_v(t) \tag{2.1.2}$$

$$\omega_f(t) = \omega_{IN} - \omega_{co}(t) = \omega_I - \omega_v(t) + \omega_o \tag{2.1.3}$$

where ω_{IF} is the nominal intermediate frequency (IF), ω_I is the input offset frequency, ω_o is the STT resonant frequency and $\omega_v(t)$ is the VCO frequency offset from its zero input frequency. The input offset frequency, ω_I, is assumed to be a constant during any TDMA burst but takes on any value in the range $\pm\omega_{IM}$ for each burst.

In Figure 2.4, the frequency variables and the loop model are simplified again by removing all constant frequency components which are not necessary for analysis. The VCO offset frequency, $\omega_v(t)$, is subtracted from the input offset frequency, ω_I, to get the frequency detector input error frequency $\omega_e(t)$. Without a hard limiter, the frequency detector or STT input $v_i(t)$ is:

$$v_i(t) = A \cos(\omega_o t + \theta_e(t)) \tag{2.1.4}$$

where $\dot{\theta}_e(t) = \omega_e(t)$

With a hard limiter, the STT input $v_i(t)$ is:

$$v_i(t) = B \operatorname{sgn}\{\text{modulo}_{2\pi}[\omega_o t + \theta_e(t) + \tfrac{\pi}{2}] - \tfrac{1}{2}\} \tag{2.1.5}$$

where $\operatorname{sgn}(x) = 1$ if $x > 0$, 0 if $x = 0$, -1 if $x < 0$

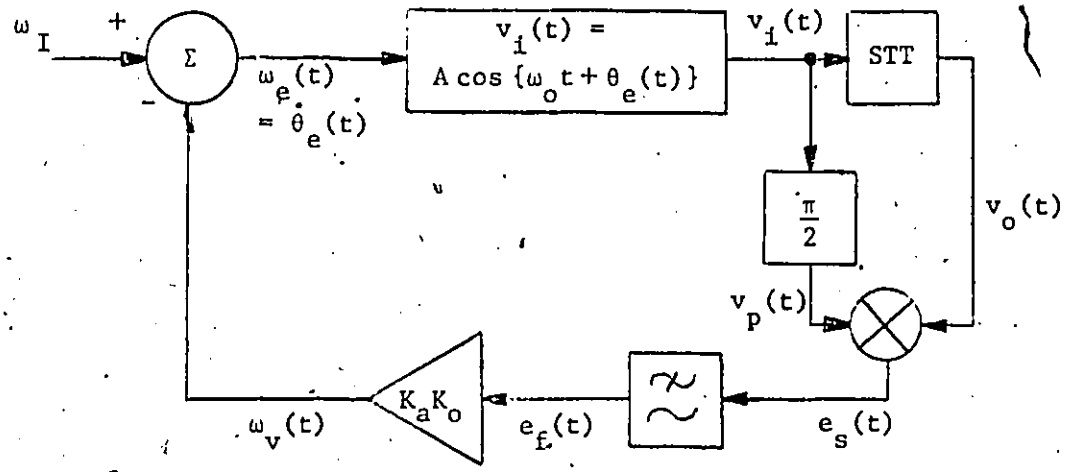

Figure 2.4 (a): Simplified Loop Model without Limiters

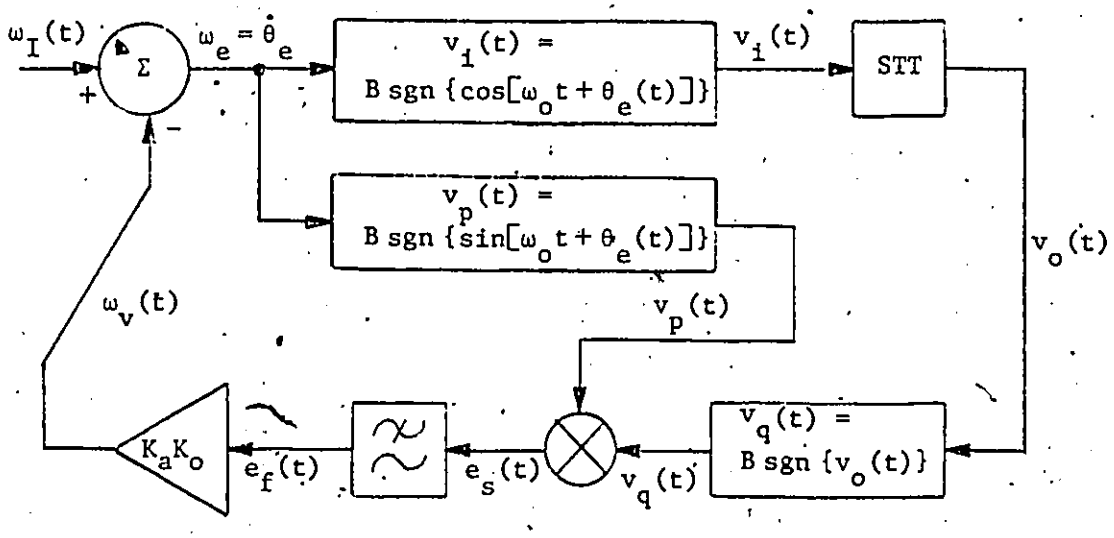

Figure 2.4(b): Simplified Loop Model with Hard Limiters

Equation (2.1.5) used for $v_i(t)$ with a hard limiter is a square wave with the same frequency and phase as equation (2.1.4) used when no hard limiter is present. The frequency detector output, $e_s(t)$, is filtered by a loop low-pass filter (LPF) to obtain the filtered error signal, $e_f(t)$. A first order LPF with transfer function,

$$F(s) = \frac{1}{\tau_f s+1} \tag{2.1.6}$$

is assumed where τ_f is the LPF time constant. The VCO offset frequency, $\omega_v(t)$, is then given by:

$$\omega_v(t) = K_a K_o \; e_f(t) \tag{2.1.7}$$

where K_a is the amplifier gain and K_o is the VCO sensitivity (rad/s/volt). This equation implies that the amplifier and VCO have infinite bandwidth, however, in practice it would only be necessary that any poles or zeroes in the amplifier and VCO transfer functions be at least an order of magnitude higher in frequency than the open loop gain crossover frequency.

The only remaining relationship to be established in the loop is the error signal, $e_s(t)$, dependent on the STT input frequency error $\omega_e(t)$. This is done for steady-state operation of the STT in the next section.

2.2 Frequency Detector Steady-State Operation

The frequency detector has three components: A single-tuned resonant circuit or tank (STT); a 90^o phase shifter; and a multiplier, as shown in Figure 2.5.

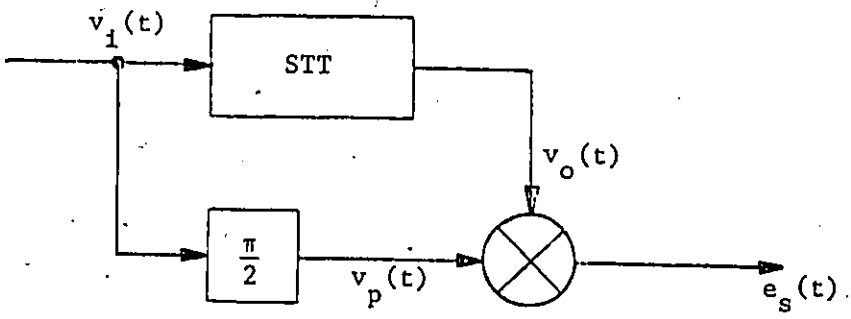

Figure 2.5 (a): Frequency Detector Model without Limiter

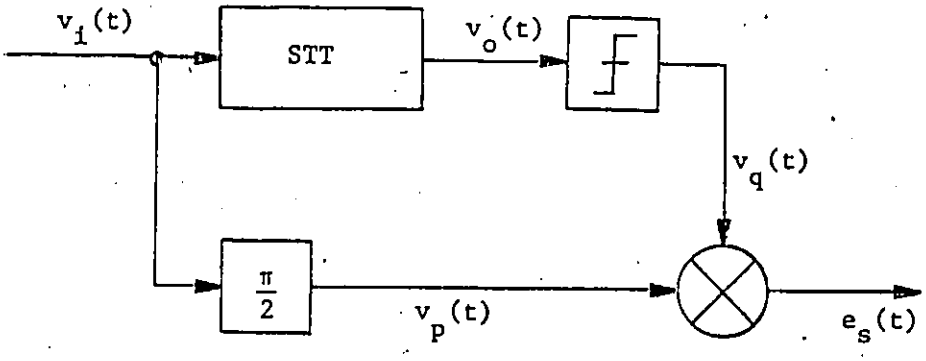

Figure 2.5 (b): Frequency Detector Model with Limiter

The STT has two purposes. First, it provides a phase shift proportional to the frequency error, $\omega_e(t)$. Second, it provides narrowband filtering of the recovered carrier. The multiplier functions as a phase detector. Since the STT has 0^o phase shift at approximately the resonant frequency, ω_o, the 90^o phase shift is required so that the phase detector output is the sine of the STT phase shift, rather than the cosine and thereby provides an error signal. There are a number of ways in which the phase shifter can be realized in practice. A two-pole, low-pass filter with its 6 dB point at ω_o is suitable or a time delay equal to $\frac{\pi}{2\omega_o}$ is suitable.

The steady-state operation of the frequency detector can be derived with the following steady-state transfer function for the STT:

$$H(j\omega) = \frac{1}{1 + jQ\left(\frac{\omega}{\omega_o} - \frac{\omega_o}{\omega}\right)} \tag{2.2.1}$$

where Q is the STT quality factor

ω_o is the STT resonant frequency

The magnitude and phase responses are:

$$|H(j\omega)|^2 = \frac{1}{1 + Q^2\left(\frac{\omega}{\omega_o} - \frac{\omega_o}{\omega}\right)^2} \tag{2.2.2}$$

$$\angle H(j\omega) = -\tan^{-1}\left[Q\left(\frac{\omega}{\omega_o} - \frac{\omega_o}{\omega}\right)\right] \tag{2.2.3}$$

The argument of the inverse tangent may be simplified for narrow-band analysis by substituting $\omega_f = \omega_o + \omega_e$ and by assuming $\omega_e << \omega_o$, as follows:

$$Q\left(\frac{\omega_f}{\omega_o} - \frac{\omega_o}{\omega_f}\right) = Q\left(\frac{\omega_e + \omega_o}{\omega_o} - \frac{\omega_o}{\omega_o + \omega_e}\right) \qquad \omega_f = \omega_o + \omega_e$$

$$= Q\left(\frac{\left(1 + \frac{\omega_e}{\omega_o}\right)^2 - 1}{1 + \frac{\omega_e}{\omega_o}}\right)$$

$$= 2Q\left(\frac{\omega_e}{\omega_o}\right)\left(\frac{1 + \frac{\omega_e}{2\omega_o}}{1 + \frac{\omega_e}{\omega_o}}\right)$$

$$Q\left(\frac{\omega_f}{\omega_o} - \frac{\omega_o}{\omega_f}\right) = \tau\omega_e \qquad \omega_e << \omega_o \tag{2.2.4}$$

where $\tau = \frac{2Q}{\omega_o}$

Assuming for the moment that the STT is in steady state, the values for $v_i(t)$ $v_o(t)$ and $v_p(t)$ from Figure 2.5 may be written as:

$$v_i(t) = A \cos\left[(\omega_e(t) + \omega_o)\ t\right] \tag{2.2.5}$$

$$v_o(t) = A\ |H(j\omega)| \cos\left[(\omega_e(t) + \omega_o)\ t + \angle H(j\omega)\right] \tag{2.2.6}$$

$$v_p(t) = A \sin\left[(\omega_e(t) + \omega_o)\ t\right] \tag{2.2.7}$$

The steady-state error signal, e_{ss}, (difference frequency only) is:

$$e_{ss} = -\frac{1}{2} A^2\ |H(j\omega)|\ \sin\left[\angle H(j\omega)\right] \tag{2.2.8}$$

$$= \frac{-\frac{1}{2} A^2}{\sqrt{1 + \tau^2 \omega_{es}^2}} \sin\left[-\tan^{-1} \tau\omega_{es}\right] \qquad \omega_{es} << \omega_o \tag{2.2.9}$$

$$e_{ss} = \frac{\frac{1}{2} A^2 \tau\omega_{es}}{1 + \tau^2 \omega_{es}^2} \qquad (2.2.10)$$

where ω_{es} is the steady-state value of ω_e

If a hard limiter is used after the STT, the magnitude component of $H(j\omega)$ is removed from the error signal and the denominator of (2.2.10) would be raised to an exponent of $\frac{1}{2}$ as shown in Figure 2.6.

If a hard limiter is used before the frequency detector, the result is approximately the same, except that the signal amplitude A is replaced by the limiter output amplitude B. This is so, because the STT essentially possess only the fundamental frequency, and the only significant term in the product of $v_o(t)$ and $v_p(t)$ is then the difference frequency component of the fundamentals. Finally, if $\tau\omega_e$ is small compared to unity, then:

$$e_{ss} \approx \frac{1}{2} A^2 \tau\omega_{es} \qquad \tau\omega_e << 1 \qquad (2.2.11)$$

The condition $\omega_e << \omega_o$ will be considered to be always true (i.e. a design constraint) so that equation (2.2.10) is always valid for steady state. The condition $\tau\omega_e << 1$ may also be included as a design constraint, however, it is left for further consideration as a constraint since other factors such as noise, pattern jitter and acquisition time may affect the merits of doing so. It will be assumed that the condition

$$\tau\omega_{es} << 1 \qquad (2.2.12)$$

will always be true.

In practice, the steady-state error signal e_{ss} will be assumed to be related to ω_{es} as:

$$e_{ss} = K_d \tau\omega_{es} \qquad (2.2.13)$$

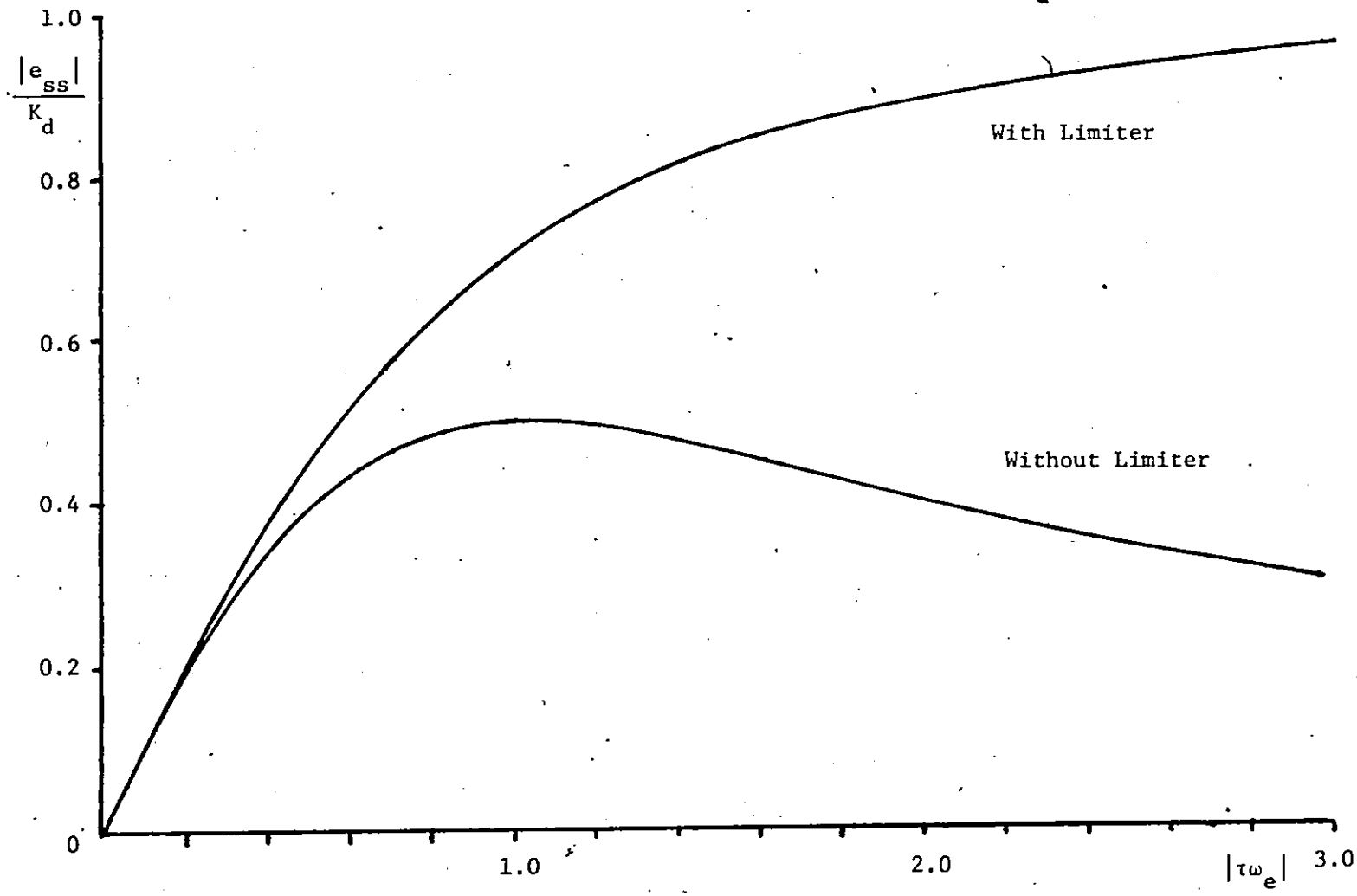

Figure 2.6: Error Signal (e_{ss}) Output vs. $\tau\omega_e$ with and without a Limiter in Frequency Detector

where K_d is the phase detector sensitivity in volts/rad. For purposes of standardizing results, K_d will be assumed to be equal to one.

While discussing the steady-state operation of the frequency detector, it is also important to consider the time required to reach steady state. This is important because the loop might be approximated by a single first-order linear differential equation if $\tau\omega_e << 1$ and the STT time constant is very small compared to the loop response time. The STT impulse response, h(t), is:

$$h(t) = \frac{2}{\tau} u(t)\, e^{-\frac{t}{\tau}} \left[\cos \omega_d t - \left(\frac{1}{\tau\omega_d}\right) \sin \omega_d t\right] \qquad (2.2.14)$$

where $\tau = \frac{2Q}{\omega_o}$ is the STT time constant and ω_d is the damped natural frequency of the STT. Since the effect of an impulse at the STT input will die out after approximately 5τ secs., the effect of any change in input will die out after 5τ secs. Hence, not only does τ determine the error signal sensitivity but also, it gives the transient time for any change through the STT.

2.3 Linear Operation of FLL

A linear model for the FLL can be formulated as shown in Figure 2.7 by making two restrictions. First, the STT must be in steady state so that:

$$e_{ss} = \frac{\tau\omega_{es}}{1 + \tau^2 \omega_{es}^2} \qquad K_d = \frac{1}{2} A^2 = 1 \qquad (2.3.1)$$

Second, the restriction, $\tau\omega_e << 1$ simplifies equation (2.3.1) so that it is linear. The steady-state requirement is very restrictive since

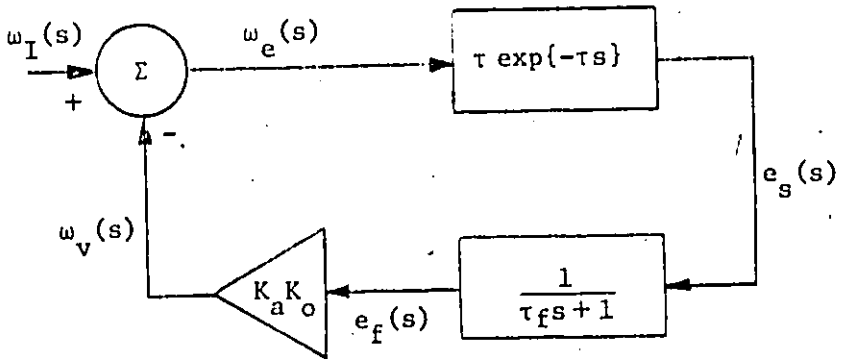

Figure 2.7 (a): Linear Loop Model for $\tau\omega_e(s) << 1$ and $|s| << \omega_o$

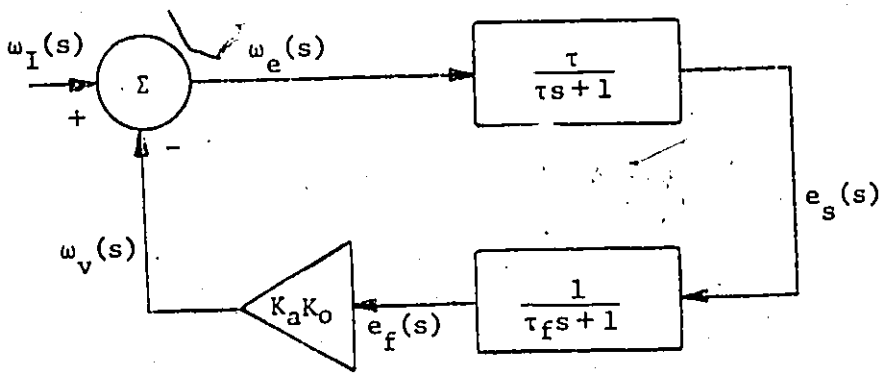

Figure 2.7 (b): Linear Loop Model for $\tau\omega_e(s) << 1$

to be in steady state, the input quantity, $\omega_e(t)$ must be constant. This steady-state requirement may be relaxed slightly by using an approximation from reference [5]. As long as $\omega_e(t)$ has amplitude much less than $\frac{1}{\tau}$ and is restricted to a bandwidth W where $W << \omega_o$, then:

$$e_s(t) \simeq \tau\omega_e(t-\tau) \qquad \begin{array}{l} \omega_e(t) << \frac{1}{\tau} \\ \omega_e(j\omega) \simeq 0, \ |\omega| > w, \end{array} \tag{2.3.2}$$

If the STT input $v_i(t)$ is thought of as a frequency modulated carrier, then these relaxed restrictions are equivalent to stating that the carrier has maximum frequency deviation much less than $\frac{1}{\tau}$ and maximum bandwidth much less than ω_o. With the above restrictions in mind, then the loop response may be obtained with the following three equations:

$$\omega_v(s) = K_v e_f(s) = K_v F(s)\, e_s(s) \tag{2.3.3}$$

$$e_s(s) \simeq \tau \exp\{-s\tau\}\, \omega_e(s) \tag{2.3.4}$$

$$\omega_e(s) = \omega_I(s) - \omega_v(s) \tag{2.3.5}$$

where F(s) is the LPF transfer function, $K_v = K_a K_o K_d$ and $K_d = 1$. The input frequency offset to frequency error transfer function is then:

$$\frac{\omega_e(s)}{\omega_I(s)} \simeq \frac{1}{1 + K_v \tau e^{-\tau s} F(s)} \tag{2.3.6}$$

with the restrictions,

$$\omega_I(s) << \frac{1}{\tau} \tag{2.3.7}$$

$$|s| << \omega_o \tag{2.3.8}$$

Substituting for F(s) (equation 2.1.6) gives:

$$\omega_e(s) \simeq \left[\frac{\tau_f s + 1}{\tau_f s + 1 + K_v \tau \exp\{-\tau s\}}\right] \omega_I(s) \qquad (2.3.9)$$

The exponential factor exp $\{-\tau s\}$ in the denominator is not significant if:

$$|s| << \frac{1}{\tau} \qquad (2.3.10)$$

$$\tau_f >> K_v \tau^2 \qquad (2.3.11)$$

Then for an initial frequency offset, ω_I (in zero state and at t = 0), the error frequency time response is:

$$\omega_e(t) \simeq \left(\frac{1}{1 + K_v \tau}\right) (1 + K_v \tau \exp\{-\frac{t}{\tau_c}\}) \qquad (2.3.12)$$

where

$$\tau_c = \frac{\tau_f}{1 + K_v \tau} \qquad (2.3.13)$$

with restrictions of inequalities (2.3.7), (2.3.10) and (2.3.11). Using equation (2.3.13), inequality (2.3.11) may be restated as:

$$\tau_c >> \tau \qquad (2.3.14)$$

A more general way of handling the error signal detector in a linear loop model is to assume only that the maximum frequency deviation of $v_d(t)$ (maximum value of $\omega_e(s)$) is small compared to the bandwidth of the STT, so that the frequency output of the STT, $\omega_o(s)$, is linearly related to input and may be written [16] as:

$$\omega_o(s) = H_b(s)\ \omega_e(s) \qquad \omega_e(s) << \frac{1}{\tau} \tag{2.3.15}$$

or in terms of phase:

$$\theta_o(s) = H_b(s)\ \theta_e(s) \tag{2.3.16}$$

where $H_b(s)$ is the low-pass equivalent of H(s) which is the STT transfer function. Since the 3 dB bandwidth $(\frac{2}{\tau})$ of H(s) is twice that of $H_b(s)$, then:

$$H_b(s) = \frac{1}{\tau s + 1} \tag{2.3.17}$$

One way of appreciating the low deviation restriction is to remember that frequency modulation is approximately linear for small modulation index (low deviation), and has only significant levels of the first sidebands of the baseband frequency. With only the first sidebands then equations (2.3.15) and (2.3.16) are valid for any value of s. With equation (2.3.16) the error signal, $e_s(s)$, may be written as:

$$\begin{aligned} e_s(s) &= \theta_e(s) - \theta_o(s) \\ &= (1 - H_b(s))\ \theta_e(s) \\ &= \left(\frac{\tau s}{\tau s + 1}\right)\ \theta_e(s) \\ e_s(s) &= \tau H_b(s)\ \omega_e(s) \end{aligned} \tag{2.3.18}$$

since $\omega_e(s) = s\theta_e(s)$. Equation (2.3.18) is consistent with equation (2.3.4) since the first two terms of the series expansion of exp $\{-\tau s\}$ equal $H_b(s)$, however, equation (2.3.18) is more general.

By using equation (2.3.18) with equations (2.3.3) and (2.3.5), the transfer function between $\omega_I(s)$ and $\omega_e(s)$ is:

$$\frac{\omega_e(s)}{\omega_I(s)} = \frac{1}{1 + K_v\tau\ H(s)\ F(s)}$$

$$= \frac{\omega_n^2\ (\tau s+1)\ (\tau_f s+1)}{(1 + K_v\tau)\ (s^2 + 2\delta\omega_n s + \omega_n^2)} \qquad (2.3.19)$$

where $2\delta\omega_n = \frac{1}{\tau}$ (2.3.20)

$$\omega_n = \sqrt{\frac{1}{\tau_c\tau}} \simeq \sqrt{\frac{K_v}{\tau_f}} \qquad (2.3.21)$$

$$\delta = \frac{1}{2}\sqrt{\frac{\tau_c}{\tau}} \simeq \frac{1}{2}\sqrt{\frac{\tau_f}{K_v\tau^2}} \qquad (2.3.22)$$

and the first-order loop time constant, τ_c, is given by equation (2.3.13). The error frequency time response, $\omega_e(t)$ for a step input, $\omega_I(s) = \frac{\omega_I}{s}$, and for $0 < \delta < 1$ is:

$$\omega_e(t) \simeq \left(\frac{\omega_I}{1+k_v\tau}\right)\left[1 + K_v\tau \exp\left(-\frac{t}{2\tau}\right)\ \frac{\sin\ \phi(t)}{D}\right] \qquad (2.3.23)$$

where $D = \sqrt{1-\delta^2}$ (2.3.24)

$$\phi(t) = \omega_n D t - \tan^{-1}\left(-\frac{D}{\delta}\right) \qquad (2.3.25)$$

Equation (2.3.23) is completely valid for $0 < \delta < 1$ as long as the frequency deviation of $v_i(t)$ is small. As the deviation increases, equation (2.3.18) becomes invalid as the STT's effect on the frequency modulation becomes nonlinear. In Chapter 3, the linear model of equation

(2.3.23) will be compared to an exact differential equation solution.

2.4 Identification of Significant Loop Parameters

There are three significant parameters in the FLL, namely, the STT time constant or mid-band group delay, τ, the error signal gain, K_v, and the loop filter time constant, τ_f. In the following, the significance of these three parameters is demonstrated.

The filtered error signal $e_f(t)$ at steady state is:

$$e_{fs} = K_d \tau \omega_{es}, \qquad F(0) = 1 \tag{2.4.1}$$

The steady state VCO relative offset frequency ω_{vs} is then:

$$\omega_{vs} = K_a K_o K_d \tau \omega_{es} \tag{2.4.2}$$

The error signal gain, K_v, is then defined as:

$$K_v = K_a K_o K_d \quad (s^{-1}) \tag{2.4.3}$$

At steady state then the ratio of the frequency error, ω_{es}, to the constant input frequency offset, ω_I, is:

$$\frac{\omega_{es}}{\omega_I} = \frac{1}{1 + K_v \tau} \tag{2.4.4}$$

The quantity $K_v \tau$ is referred to as the open loop gain, K_{oL}. In practice, K_{OL} is much greater than one and,

$$K_{oL} = K_v \tau \simeq 1 + K_v \tau \tag{2.4.5}$$

The steady-state phase error introduced by the FLL on the recovered carrier is then:

$$\theta_{es} = \tau \omega_{es} = \frac{\tau \omega_I}{1 + K_v \tau} \simeq \frac{\omega_I}{K_v} \tag{2.4.6}$$

The STT 3 dB bandwidth, ω_3, is:

$$\omega_3 \simeq \frac{\omega_o}{Q} = \frac{2}{\tau} \qquad Q >> 1 \tag{2.4.7}$$

The linear models of equations (2.3.12) and (2.3.23) predict that the acquisition time (to be defined explicitly in Chapter 3) of the loop is proportional to τ_c, if $\tau_c >> \tau$; and as the value of τ_c approaches the value of τ, the acquisition time would become proportional to τ. Since τ_c is only dependent on τ_f, K_v and τ, then the acquisition time is only dependent on τ, τ_f and K_v. Thus, the operation of the FLL can be solely related to the three parameters, τ, K_v, and τ_f.

In practice, it is desirable to have several ways of measuring the critical parameters of a system, in order to double check measurements, or in the case that one method is impractical.

The STT time constant, τ, can be measured in several ways:

1) $$\tau = \frac{2}{\omega_3} = \frac{2Q}{\omega_o} \tag{2.4.8}$$

where ω_3 is the STT 3 dB bandwidth

2) $$\tau = \pm \frac{1}{\omega_{em}} \tag{2.4.9}$$

where ω_{em} is error frequency at which maximum error signal occurs. (See Figure 2.6).

$$3)\quad \tau = \frac{d\angle H(j\omega)}{d\omega}\ \Big|\ \omega = \omega_o \qquad (2.4.10)$$

which is the STT mid-band group d[redacted]

The open loop gain, K_{OL}, is easily measured by taking the ratio of the steady-state error frequency, ω_{es}, and the input frequency offset, ω_I

$$K_{oL} = 1 + K_v\tau = \frac{\omega_I}{\omega_{es}} \simeq K_v\tau \qquad (2.4.11)$$

The loop filter time constant, τ_f, is:

$$\tau_f = \frac{1}{\omega_L} \qquad (2.4.12)$$

where ω_L is the low-pass filter 3 dB bandwidth, and is easily measured.

In closing this chapter, it should also be pointed out that τ, K_v and τ_f are three independently variable parameters all under the control of the system designer. The exact relationships among them are explored further in Chapter 3.

CHAPTER 3

ACQUISITION BEHAVIOUR

3.1 Introduction

The acquisition behaviour of the FLL has been analyzed in reference [1] using a simulation approach. It is proposed here to derive an exact differential equation model for the FLL and to solve it using numerical integration to obtain the loop's transient response. Very recently, Miller Communications Systems Limited (MCS) has built an FLL into their "SLIM TDMA" ground stations, as described in references [2] and [3]. It is intended to use the same or similar parameter values as MCS so that the theoretical responses obtained here can be compared with the measured responses obtained by MCS. The parameter values used in the numerical integration were:

$$\omega_o = 2\pi\ (20 \times 10^6)\ \text{rad/s}$$

$$\tau_f = 0.15,\ 0.015\ \text{ms}$$

$$Q = 67,\ 174$$

$$K_v = 30 \text{ to } 75\ \text{dB}$$

where the parameters have been defined in Chapter 2.

The transient response is primarily obtained starting with a

zero initial state for the loop. The input signal which is zero for $t < 0$ has a constant offset ω_I from the STT resonant frequency ω_o. In practice though, there would never be a zero state situation either because of noise present or because of change stored in the STT due to a previous burst.

A signal of noise and no carrier that was passed through a AGC and a hard limiter would have almost constant amplitude and phase or frequency noise determined by the quadrature component of the input noise and the channel bandwidth. After the STT, the phase or frequency noise present could be reduced to the bandwidth of the STT. The loop low-pass filter would filter the error signal variations to a $\frac{1}{2\pi\ (.15\ \text{ms})} =$ 1 kHz rate. In this instance then the STT output would be essentially a sinusoid at the normal steady-state amplitude with a random low-deviation frequency modulation of approximately 1 kHz bandwidth. The average frequency would be approximately ω_o and in this case then the initial values of the state variables when a carrier was added to the noise would correspond to that of a steady-state situation of carrier present with small frequency offset.

The undecayed remains of a past burst will also cause non-zero state initial values. The worst case would be to assume initial values which were steady-state values for the maximum expected frequency offset in the opposite sense to the newly applied carrier. This case is a worse situation than the all-noise case since here the filtered error signal $e_f(t)$ is the furthest away from its desired final value. To consider the worst case situation for acquisition, then one would use initial state variable values corresponding to the maximum expected

opposite-sense frequency offset.

After thinking about these practical situations, one might be tempted to study transient responses from other than zero initial state. However, since these practical situations were not considered initially and since to do other than zero state response when comparing various models for validity would add complication, almost all transient responses are calculated assuming zero initial state. The response of one model was calculated for the worst-case situation described in the preceding paragraph to determine what the difference would be.

3.2 Various Models Considered

Several different differential equation models have been formulated to determine the transient response of an FLL. These models vary according to the type of 90° phase shifter used, according to whether a baseband equivalent or actual bandpass model is used for the STT, and according to whether or not a hard limiter is used before the STT. The actual models considered are:

a) A bandpass model for the STT with an ideal 90° phase shifter. This model is referred to as the BPI model.

b) A bandpass STT model using a two-pole low-pass filter as a 90° phase shifter. This is referred to as the BPL model.

c) A BPL model with a hard limiter added before the STT. This is referred to as a BPLH model.

d) A BPI model with a hard limiter added before the STT. This is referred to as a BPIH model.

e) A BPI model with a hard limiter before and after the STT. This is referred to as the BPHH model.

f) A baseband model for the STT with an ideal phase shifter. This is referred to as the BB model.

Only two types of differential equations are required for all of these models. One is the equation for a STT circuit and the second is the equation of a low-pass circuit.

A STT circuit diagram is shown in Figure 3.1. Since there are two reactive elements, two first-order differential equations are required for its input-output response. These equations are (cf. Figure 3.1):

$$\dot{v}_o(t) = \frac{\omega_o}{Q} (-v_o(t) - v_c(t) + v_i(t)) \qquad (3.2.1)$$

$$\dot{v}_c(t) = \omega_o Q\, v_c(t) \qquad (3.2.2)$$

where $v_i(t)$ input voltage
$v_c(t)$ capacitor voltage
$v_o(t)$ output voltage
ω_o STT resonant frequency
Q STT quality factor

A single-pole low-pass filter is shown also in Figure 3.1. It requires a single first-order differential equation.

$$\dot{v}_{lo}(t) = \omega_L (-v_{lo}(t) + v_{li}(t)) \qquad (3.2.3)$$

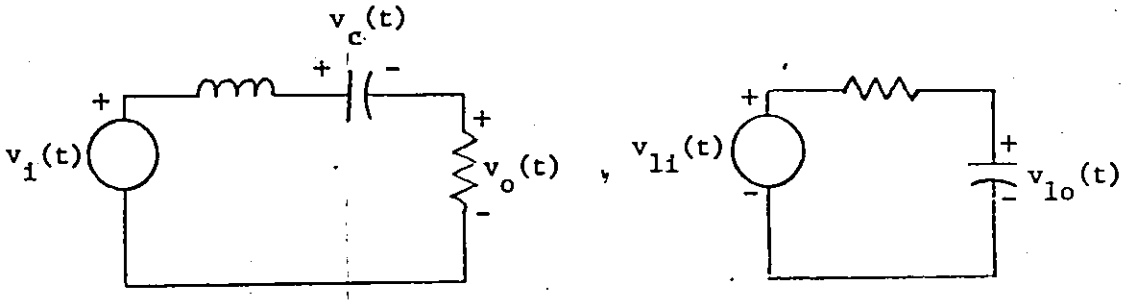

$$\dot{v}_o(t) = \frac{2}{\tau}\,(-\,v_o(t) - v_c(t) + v_i(t))$$

$$\dot{v}_c(t) = \omega_o\, Q\, v_c(t)$$

$$\dot{v}_{lo}(t) = \omega_L\,(-\,v_{lo}(t) + v_{li}(t))$$

Figure 3.1: Circuit Diagrams for STT and Low Pass Filter

where $v_{1i}(t)$ is input voltage

$v_{1o}(t)$ is output voltage

ω_L is steady-state half-amplitude frequency

These three equations are the only differential equations required for any of the six models described.

The STT input signal has two forms depending on whether or not a hard limiter is assumed. Without a hard limiter, the STT input signal $v_i(t)$ is:

$$v_i(t) \quad A \cos [\omega_o t + \theta_e(t)] \tag{3.2.4}$$

with $A = \sqrt{2}$

and $\dot{\theta}_e(t) = \omega_I - K_v e_f(t)$

For a baseband model, ω_o is set to zero. A is set to $\sqrt{2}$ so that the difference frequency error signal at steady state is (cf. Chapter 2)

$$e_{ss} = \tau\omega_{es}$$

and the loop gain is then

$$K_v = K_a K_o$$

With a hard limiter, the input signal is assumed to be:

$$v_i(t) = B \text{ sgn } \{\text{modulo}_{2\pi}\{\omega_o t + \theta_e(t) + \tfrac{\pi}{2}\} - \tfrac{1}{2}\} \tag{3.2.5}$$

where $B = \dfrac{\pi}{2\sqrt{2}}$ implies $e_{ss} = \tau\omega_{es}$

Equation (3.2.5) is a bipolar square wave of amplitude B with zero crossings in the same direction and at the same time as a cosine wave. If an ideal hard-limited sine wave is desired, then:

$$v_i(t) = B \text{ sgn } \{\text{modulo}_{2\pi}\{\omega_o t + \theta_e(t)\} - \frac{1}{2}\} \qquad (3.2.6)$$

Equation (3.2.5) is used in the ensuing analysis.

3.3 Model Equations

3.3.1 BPI Model

The state equations for this model, which assumes a band-pass STT with ideal phase shifter may be written as:

$$v_i(t) = \sqrt{2} \cos (\theta_e(t) + \omega_o t) \qquad (3.3.1)$$

$$v_p(t) = \sqrt{2} \sin (\theta_e(t) + \omega_o t) \qquad (3.3.2)$$

$$\dot{v}_o(t) = \frac{2}{\pi} [-v_o(t) - v_c(t) + v_i(t)] \qquad (3.3.3)$$

$$\dot{v}_c(t) = \omega_o Q \, v_c(t) \qquad (3.3.4)$$

$$e_s(t) = -v_o(t) \, v_q(t) \qquad (3.3.5)$$

$$\dot{e}_f(t) = \frac{1}{\tau_t} (-e_f(t) + e_s(t)) \qquad (3.3.6)$$

$$\dot{\theta}_e(t) = \omega_I + K_v e_f(t) \qquad (3.3.7)$$

where $v_o(t)$ is the STT output voltage

$v_c(t)$ is the STT capacitor voltage

$e_f(t)$ is the loop filter output voltage

$\theta_e(t)$ is the STT input phase

$v_i(t)$ is the STT input voltage

$v_p(t)$ is the phase shifter output voltage

3.3.2 BPL Model

The BPL model uses equations (3.3.1), (3.3.3), (3.3.4), (3.3.6) and (3.3.7) plus the following three equations:

$$\dot{v}_e(t) = \omega_o \left(-v_e(t) + \sqrt{2}\, v_o(t)\right) \tag{3.3.8}$$

$$\dot{v}_p(t) = \omega_o \left(-v_p(t) + \sqrt{2}\, v_e(t)\right) \tag{3.3.9}$$

$$e_s(t) = v_p(t)\, v_i(t) \tag{3.3.10}$$

where $v_e(t)$ is output voltage of first 45° phase shifter

$v_p(t)$ is the phase shifter output voltage

3.3.3 BPLH Model

The BPLH model uses the same equations as the BPL model except the STT input voltage is hard limited and the input equation is changed to:

$$v_i(t) = \frac{\pi}{2\sqrt{2}} \operatorname{sgn}\left\{\text{modulo}_{2\pi}\left\{\omega_o t + \theta_e(t) + \frac{\pi}{2}\right\} - \frac{1}{2}\right\} \tag{3.3.11}$$

3.3.4 BPIH Model

The BPIH model is the same as the BPI model except that the STT input voltage is hard limited and the STT input and the PD input voltages

change to:

$$v_i(t) = \frac{\pi}{\sqrt{8}} \operatorname{sgn} \{\text{modulo}_{2\pi}\{\omega_o t + \theta_e(t) + \frac{\pi}{2}\} - \frac{1}{2}\} \quad (3.3.12)$$

$$v_p(t) = \frac{\pi}{\sqrt{8}} \operatorname{sgn} \{\text{modulo}_{2\pi}\{\omega_o t + \theta_e(t)\} - \frac{1}{2}\} \quad (3.3.13)$$

3.3.5 BPHH Model

This model is the same as the BPIH except that a hard limiter is placed between the STT and PD. This changes the error signal, $e_s(t)$, (equation (3.12)) to the following:

$$e_s(t) = \operatorname{sgn} \{v_o(t)\} v_p(t) \quad (3.3.14)$$

3.3.6 BB Model

A baseband model for the STT was obtained by using a complex baseband representation for the input signal with respect to ω_o and using a complex low-pass filter with real coefficient $\frac{\omega_o}{2Q}$. The error signal is analytically derived from the product of the real STT output and the real phase shifted signal. The complex input signal and STT differential equations are:

$$v_{iB}(t) = \sqrt{2} (\cos \theta_e(t) + j \sin\theta_e(t)) \quad (3.3.15)$$

$$\dot{v}_{oB}(t) = \frac{\omega_o}{2Q} (-v_{oB}(t) + v_{iB}(t)) \quad (3.3.16)$$

where $v_{iB}(t)$ and $v_{oB}(t)$ are the complex input and output signals.

The error signal is derived by multiplying the real $\frac{\pi}{2}$ phase shifted input with the real STT output. The real signals are:

$$v_o(t) = R_e \{v_{oB}(t)\ e^{j\omega_o t}\}$$
$$= R_e \{v_{oB}(t)\ \cos \omega_o t - \mathrm{Im}\{v_{oB}(t)\} \sin \omega_o t \quad (3.3.17)$$

$$v_p(t) = R_e \{(\sin \theta_e(t) - j \cos \theta_e(t))\ e^{j\omega_o t}\}$$
$$= \sin \theta_e(t) \cos \omega_o t + \cos \theta_e(t) \sin \omega_o t \quad (3.3.18)$$

The error signal output is:

$$e_s(t) = -v_o(t)\ v_p(t)$$
$$= -R_e \{v_{oB}(t)\} \sin \theta_e(t) + \mathrm{Im}\{v_{oB}(t)\} \cos \theta_e(t) \quad (3.3.19)$$

The coefficient $\frac{\omega_o}{2Q}$ is derived from the fact that the equivalent low-pass filter has 3 dB bandwidth equal to half the STT 3 dB bandwidth.

In summarizing then, the equations for the BB model can be written as:

$$v_{iB}(t) = \sqrt{2}\ (\cos \theta_e(t) + j \sin \theta_e(t)) \quad (3.3.20)$$

$$\dot{v}_{oB}(t) = \frac{\omega_o}{2Q}\ (-v_{oB}(t) + v_{iB}(t)) \quad (3.3.21)$$

$$e_s(t) = \mathrm{Im}\{v_{oB}(t)\} \cos \theta_e(t) - R_e\{v_{oB}(t)\} \sin \theta_e(t) \quad (3.3.22)$$

$$\dot{e}_f(t) = \frac{1}{\tau_f}\ (-e_f(t) + e_s(t)) \quad (3.3.23)$$

$$\dot{\theta}_e(t) = \omega_I + K_v e_f(t) \qquad (3.3.24)$$

where $v_{iB}(t)$ and $v_{oB}(t)$ are complex.

3.4 Discussion of Computer Methods Used

The differential equation models were solved by numerical integration using the Runge-Kutta-Gill method. The step size used was 0.05 ns for the bandpass models and 10 ns for the baseband models. We first attempted to do the integration on a Floating Point Systems (FPS) AP120B array processor to achieve high speed but the solution tended to explode at any step size due to either errors in using the cosine function or in range reduction for the cosine argument. The AP120B has a 38-bit word with a 28-bit mantissa and 10-bit exponent. The same difficulty also occurred on the HP1000 with a 16-bit word. With a 64-bit word on the HP1000, the "blow up" problem occurred only rarely with the BPL model only. It was later realized that if the cosine argument in the model inputs were calculated in cycles rather than in radians range reduction would only require taking the fractional part of argument rather than dividing by 2π. The models which used hard limiters did not exhibit any blow up problems at all on the HP1000.

Since most runs were done for a total time period of 10 μs and the step size for the bandpass models was 0.05 μs a total of 200,000 iterations were required. On the HP1000 with maximum word size (64 bits), the solution took approximately 30 minutes for the bandpass models. The baseband models required less than a minute.

The hard limiter models were also tried on the FPS AP120B without success. It was unfortunate since at the same step size and total integration period and using the identical integration routine the AP120B took 25 s compared to 30 minutes on the HP1000. The new high precision FPS 164 array processor would handle the entire problem quite well in under 30 s.

For all plots of the error signal response and the frequency error response, only 100 points of the solution are used. This was done to keep plotting time down on the dot matrix line printer which was used for hard copy results. Using 100 points does change some of the fine detail of the responses but from observing responses using more than 100 points, it does not make significant differences.

The error signal plots which appear in this chapter are not the complete error signal which contains sum and difference frequency components. Since it is desired to consider only the difference frequency component, the mixer output signal is passed through a low-pass filter of 1 MHz bandwidth for plotting purposes although the complete error signal is applied to the loop low-pass filter, as described in Section 3.2.

3.5 Discussion of Computer Solutions

There are four significant parts to the computer simulation results. First, all the models described in Section 3.2 were run from zero state. In all cases, the frequency tracking error, $\omega_e(t)$, is plotted versus time, with error signal gain, K_v, being the main parameter that is varied. The main motivation in this part (3.5.1) will

be to verify that the models are consistent. Second, one of the models is used to examine the worst case acquisition response from steady state at a maximum offset at one polarity to the maximum opposite polarity. Third, the response from one model is compared to the measured results obtained from reference [17]. Fourth, the linear Laplace transform model of Chapter 2 is compared to the differential equation solutions.

3.5.1 Comparison of Differential Equation Models

All the differential equation models except the BPHH model (two hard limiters: one before and after the STT) give almost exactly the same response for all values of the τ_c (given in equation (2.3.13)) down to approximately τ.

This agreement is demonstrated at $\tau_c = 0.9$ in Figure 3.2. The BB, BPI, BPL, BPIH, BPLH, BPHH, and linear Laplace model responses are shown in this figure. It is interesting to note that at this value of $\tau_c = \tau$ that the baseband and bandpass models agree. Also, the use of hard limiters before the STT makes no difference to the acquisition response.

At values of $\tau_c = 0.1$ the different models give slightly different results as shown in Figure 3.3. The use of hard limiters before the STT still makes little difference and the responses of the BB, BPI, BPL, BPIH and BPIH models bear a lot of resemblance. The main discrepancy is in the final values. For a 50 kHz initial offset and a 183.4 dB loop gain the final value predicted by the steady-state equation (2.2.13) is 31.8 Hz. From Figure 3.3, the final values appear to be

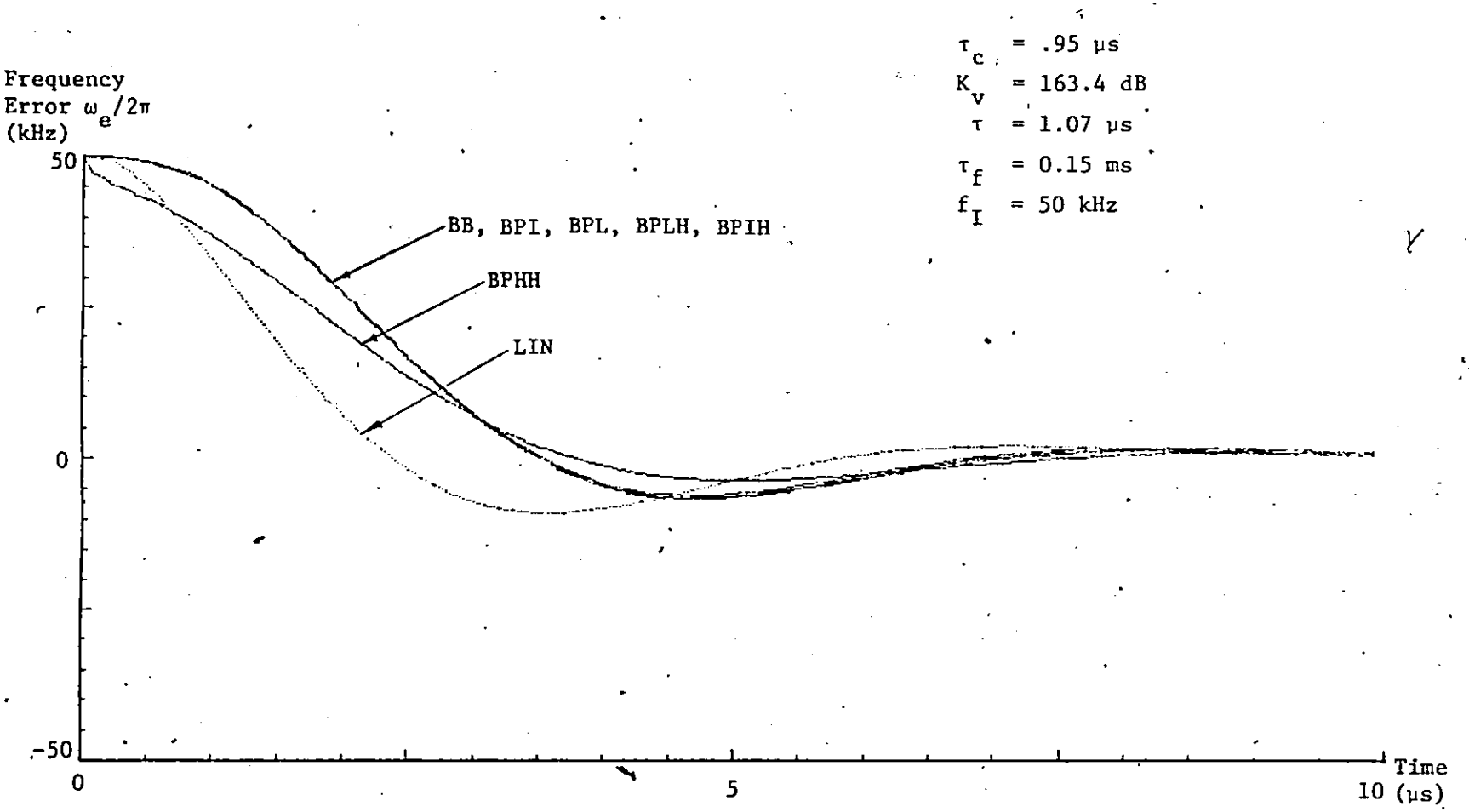

Figure 3.2: Frequency Error-Time Response
Comparison of all Models from Zero State

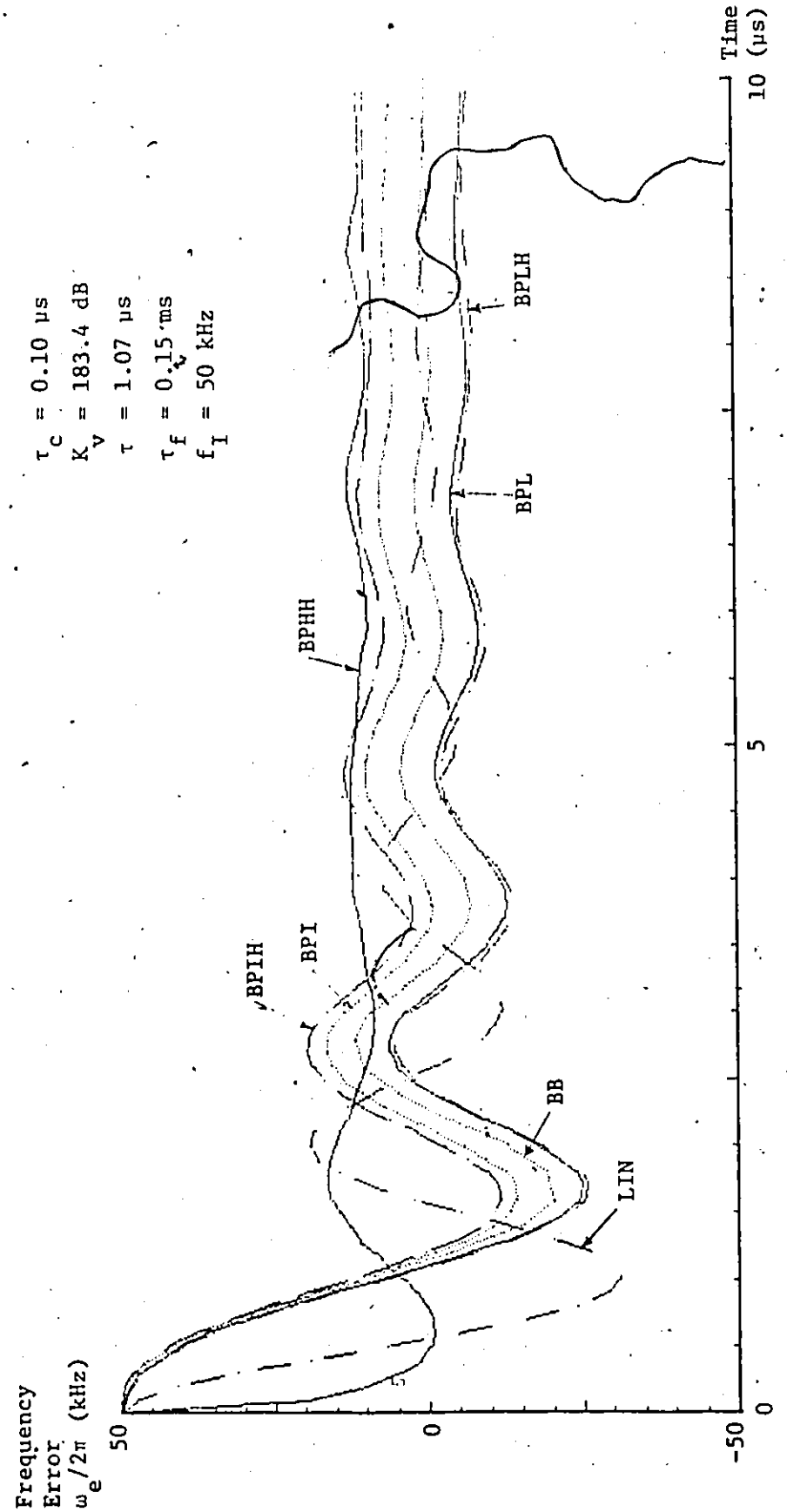

Figure 3.3: Frequency Error-Time Response
Comparison of all Models from Zero State

ranging from + 9 kHz to -6 kHz. There is no good explanation for this behaviour at present, and therefore the acquisition performance of the loop for values of τ_c much less than τ remains to be better understood, although it can be said that all models are consistent in predicting an underdamped response similar to a second-order system.

One possibility for explaining the large apparent final values is given in Appendix A. The expected final value for a constant frequency offset has a dc bias as follows:

$$e_{ss} = \frac{A^2}{2}\left(-\frac{1}{2Q} - \tau_{\omega e}\right) \qquad (3.5.1)$$

but this bias predicts ≈ 1 kHz error in the final value of the frequency error independent of K_v so that this d.c. bias cannot be the whole cause.

The responses of the BPHH model are interesting. It was not expected that this model would give the same response as the other since the steady-state frequency error response curve is different due to the second hard limiter. It might have been expected that the second limiter would reduce the order of the closed loop response, since any amplitude roll off due to the STT is removed. However, the response is still second order, but slightly faster and with slightly more damping.

One other result shown in Figure 3.4 is interesting to note. The error frequency acquisition performance is only dependent on the ratio of $\frac{K_v}{\tau_f}$ and not on the individual values. This agrees with the linear model of Section 2.3.

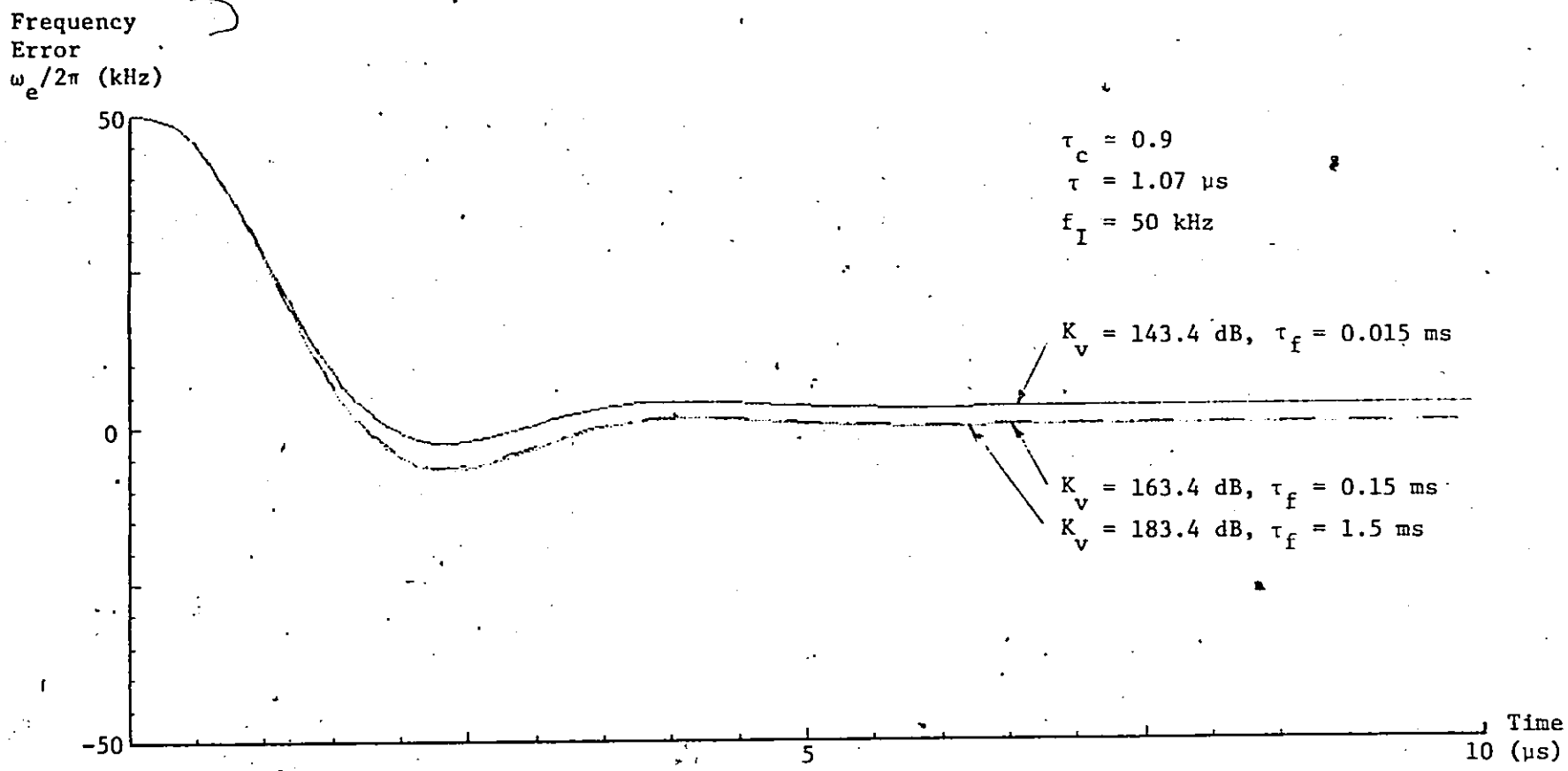

Figure 3.4: Frequency Error vs. Time Response for Various K_v and τ_f with a Constant $\frac{K_v}{\tau_f}$ Ratio using BB Model

(Note: $\tau_c = \frac{\tau_f}{1+K_v\tau} = \frac{\tau_f}{K_v\tau}$)

3.5.2 Worst-Case Non-Zero State Response

In order to examine the worst-case non-zero state response, the BPLH model was used with the same loop parameters as in Figure 3.2. Four runs were made starting at zero state with initial frequency offsets of ± 50 kHz and ± 200 kHz (± 0.3 and ± 1.25 of the STT 3 dB down frequency offsets). After 10 μs, the frequency offset was switched to the opposite polarity to simulate the worst case non-zero state acquisition. The results shown in Figure 3.5 are encouraging since the worst case non-zero state acquisition times are only about 30% greater than the non-zero state cases.

3.5.3 Comparison with Measured Results

A photograph of frequency error response was obtained from Miller Communications Systems (MCS) for a FLL with the following parameters:

$$f_I = 50 \text{ kHz}$$

$$f_o = 20 \text{ mHz}$$

$$Q = 174$$

$$\tau_f = 0.15 \text{ ms}$$

$$K_v = 145 \text{ dB}$$

The measured response is drawn in Figure 3.6 with the differential equation solution. The agreement is remarkably close, considering that the MCS system had an AGC circuit during the STT which initially provided a higher input level to the STT and would make the loop gain

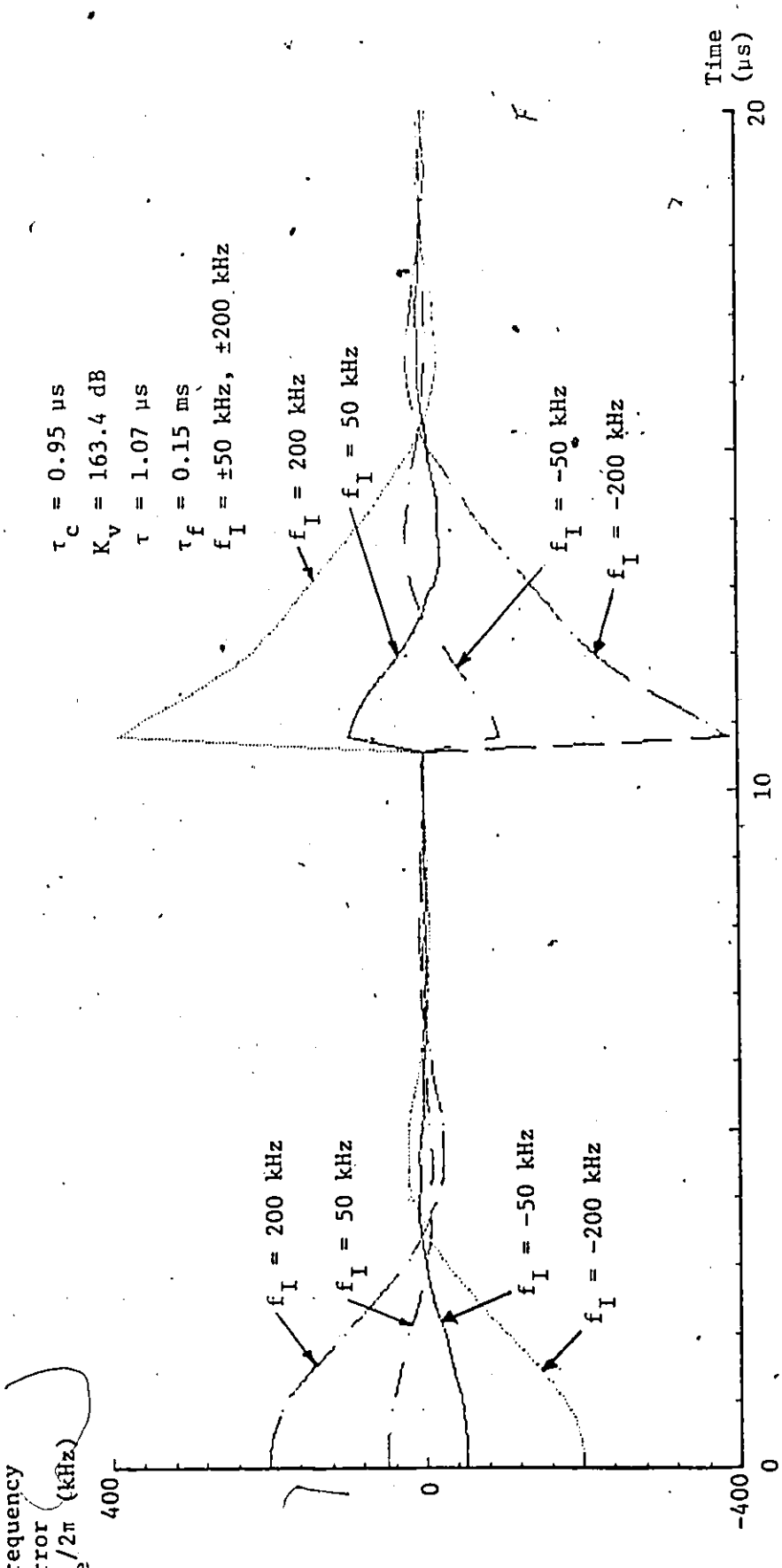

Figure 3.5 Frequency Error vs. Time Response from Zero State (t = 0) and from Steady State (t = 10.5 μs) for $+f_I$ and $-f_I$ Frequency Offsets

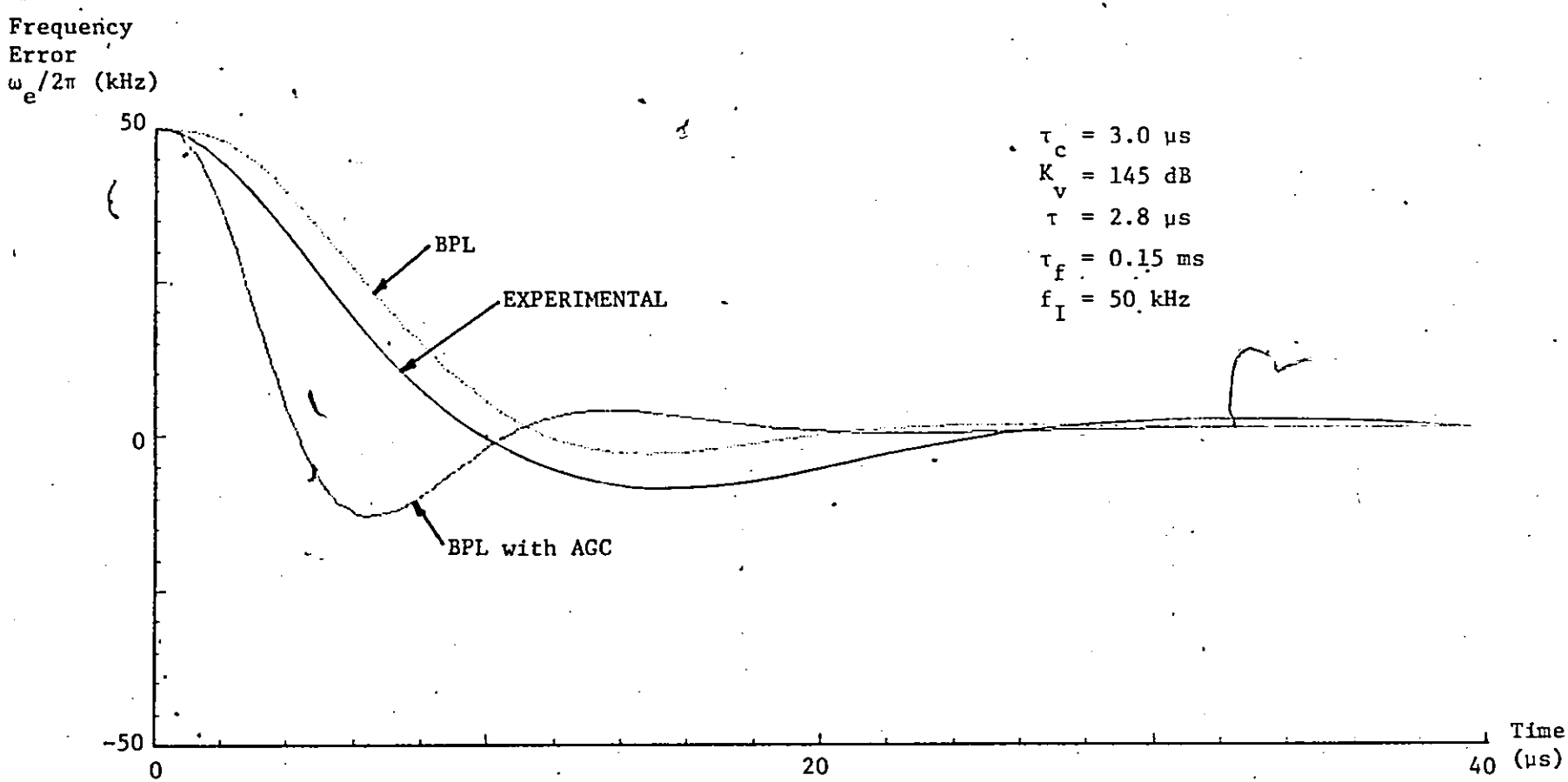

Figure 3.6: Frequency Error-Time Response for BPL Model and Measured Experimental Response

higher for a short time.

3.5.4 Comparison with Linear Model

The error frequency response calculated using the linear model of Chapter 2, equation (2.3.23), is shown in Figures 3.2, 3.3 and 3.7. The linear model predicts a first-zero crossing in about 25% shorter time and is slightly less damped, but the natural frequency and the envelope of the response are almost the same as for all the differential equation solutions. This is a very useful result because it means that even for acquisition performance the linear model may be applied, and it certainly would be useful for analyzing phase jitter performance.

3.6 Acquisition Time and Choice of Loop Parameters

Since the linear model given in Section 2.3 agrees so well with the differential equation models, equation (2.3.23) should be useful in estimating the acquisition time.

For a second-order system given by equation (2.3.19), the envelope of the time response decreases as the damping ratio decreases until critical damping where $\delta = 1$. For $\delta < 1$, the envelope is constant with respect to changes in δ. From equation (2.3.22) then the parameter τ_c should be made less than 4τ to achieve the best acquisition time for a given value of τ and the envelope of the time response in equation (2.3.23) can be used to estimate acquisition time. It is also convenient to assume that τ_c be made equal to τ which would imply $\delta = \frac{1}{2}$.

In order to estimate acquisition time, it is necessary to define the point where a suitable carrier phase estimate has been obtained. For

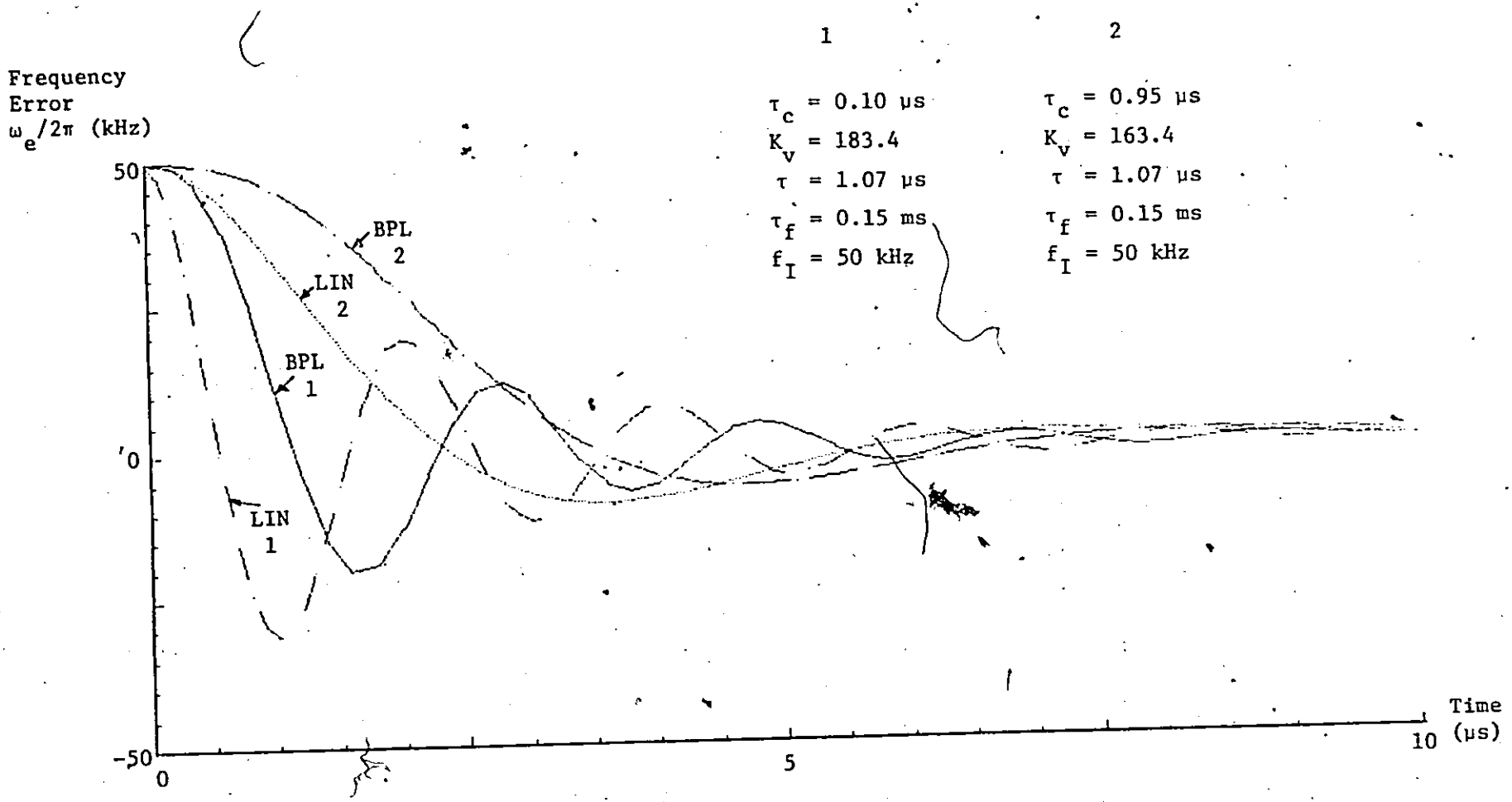

Figure 3.7: Frequency Error-Time Response for Linear and BB Model

the FLL, the carrier phase estimate error is the STT phase shift, $\theta_s(t)$. The acquisition point then is the point where the carrier phase error, $\theta_s(t)$ falls below and stays below the maximum allowable phase error, θ_{sm}, which causes the maximum tolerable degradation (however small it might be) in the bit error rate (BER) performance of the receiver. It is important not to confuse the carrier phase error θ_s, with the STT input phase $\theta_e(t)$, given in equation (3.3.7).

Now, the FLL carrier phase estimate error, θ_s, is related to the frequency tracking error, ω_e, as:

$$\theta_s \simeq \tan^{-1}(\tau\omega_e) \leq \tau\omega_e \qquad \omega_e << \omega_o \qquad Q >> 1 \tag{3.6.1}$$

Using the envelope of equation (2.3.23) and substituting $\frac{\theta_s}{\tau}$ for ω_e and rearranging the following estimate for the worst-case acquisition time, t_{aw}, can be obtained as:

$$t_{aw} \simeq 2\tau \ln\left(\frac{\tau\omega_{Im}}{\theta_{sm} - \theta_{sfm}}\right) \tag{3.6.2}$$

where ω_{Im} is the maximum value of ω_I, θ_{sm} is the maximum tolerable value of θ_s, and $\theta_{sfm} \simeq \frac{\omega_{Im}}{K_v}$ is the maximum final value of θ_s. Obviously, θ_{sm} must be larger than θ_{sfm} and ideally θ_{sfm} should be insignificant with respect to θ_{sm} in order to minimize the argument of the logarithm in equation (3.6.2). Therefore, K_v should be chosen such that:

$$K_v >> \frac{\omega_{Im}}{\theta_{sm}} \tag{3.6.3}$$

Also with τ_c assumed equal to τ then using equation (2.3.22):

$$\tau_f = K_v \tau^2 \qquad (3.6.4)$$

and all the parameters of the second order FLL are established relative to τ.

Now, the STT time constant, τ, could be chosen to obtain any value of acquisition time desired, except for several difficulties. First, as τ is decreased, the level of receiver Gaussian noise and data dependent noise in the loop will increase. Second, if the value of τ is greater than $\frac{1}{\omega_{Im}}$, then equation (3.6.2) becomes too optimistic due to the non-linear error signal versus frequency response. Therefore, in choosing τ, noise, maximum offset and acquisition time must be considered.

CHAPTER 4

NOISE AND JITTER PERFORMANCE

The effect of noise on the FLL is primarily discussed for a FLL with a hard limiter included before the STT. The justification for this is given in Section 4.1 where the equivalence of the limiter STT, PD and phase shifter to a conventional single-tuned filter and a limiter discriminator is discussed. In Section 4.2 the equivalence of the FLL to the FM Feedback (FMFB) demodulator first described by Chaffee in 1939 [7] is discussed, and the application of a linear model for high signal-to-noise case is given. The analysis of phase jitter or frequency jitter is also equivalent to the noise analysis for high SNR.

4.1 The Effect of Limiters

The STT output signal is used for two purposes. It is used as the recovered carrier, and it is also one of two inputs to the phase detector. For both uses, it is desired to have constant amplitude. The reference phase input to the phase detector also should have constant amplitude. The best place then to place a limiter would be as shown in Figure 2.3. If the hard limiter is not used, what happens is the following. Since the phase detector is a multiplier, any amplitude variation which passes through the STT to the PD (and is also present at the PD reference input), gets squared by the multiplier. Therefore, any am-

plitude variation entering the FLL will get detected and cause a d.c. bias or offset in the error signal. In Appendix A, it is shown that for a STT input signal:

$$v_i(t) = (A + n_c(t)) \cos \omega_f t - n_s(t) \sin \omega_f t$$

that the expected steady-state difference frequency error signal is given by:

$$e_{ss} = E\{\lim_{t\to\infty} e_s(t)\} = \left(\frac{A^2}{2} + \frac{N_o}{2\tau_x}\right)\left(-\frac{1}{2Q} + \tau_{\omega e}\right) \qquad (4.1.1)$$

where $\frac{N_o}{2\tau_x}$ is the white noise power contained in $v_i(t)$ and $\frac{1}{\tau_x}$ is the receiver noise bandwidth to the FLL input. The variance of the error signal without a limiter would have terms proportional to $\frac{A^2 N_o}{\tau_x}$ and $\frac{N_o^2}{\tau_x^2}$. Another problem with not using a limiter is variation in the carrier level. Even if an AGC is used prior to the FLL, the dynamics of the AGC will affect the dynamics of carrier acquisition. The ratio of the AGC wide open gain (no carrier present) to the nominal gain will depend on the noise level and it would be impossible to optimize the acquisition of the FLL. It is therefore assumed that a limiter would be used prior to the STT.

Other improvements are possible by using limiters at the STT output as shown in Figures 2.2 or 2.3. Limiters in these positions would remove any PM to AM conversion of the STT and would also allow slightly faster acquisition, as shown in Chapter 3.

The pre-STT limiter, plus STT and PD are roughly equivalent to a ideal limiter-discriminator plus a single-pole low-pass filter of 3 dB

bandwidth $\frac{1}{\tau}$. This statement is justified by the linear model equation (2.3.18) developed in Chapter 2, which was shown to be valid in Chapter 3.

4.2 Equivalence to FMFB Demodulator

The linear open-loop transfer function of the FLL is:

$$\frac{\omega_v(s)}{\omega_I(s)} = \frac{\theta_v(s)}{\theta_I(s)} = K_v \tau H_b(s)\, F(s). \tag{4.2.1}$$

where $\omega_v(s)$ is the VCO output error frequency and $H_b(s)$ and $F(s)$ are:

$$H_b(s) = \frac{1}{\tau s + 1} \tag{4.2.2}$$

$$F(s) = \frac{1}{\tau_f s + 1} \tag{4.2.3}$$

This linear model is almost the same as the linear model used by Klapper and Frankle (reference [16]). Although the application of this circuit for carrier recovery is slightly different and the performance criteria and critical parameters may be different, reference [16] (Chapter 4 and 7) has a large amount of information which may be helpful in using this approach for carrier recovery.

4.3 Linear Noise Performance

Besides the acquisition performance discussed in Chapter 3, the other critical parameter of interest is the phase error $\theta_s(s)$ between the received modulated signal and the recovered carrier caused by the

recovery loop for various perturbations such as received frequency offset, receiver front end noise, and phase noise due to reference oscillators in the up and down convertors. All of these perturbations can be lumped together (assuming high CNR) as an input phase variation $\theta_I(s)$. Ideally, the CR* circuit will track the long-term variations but not the short-term variations such as pattern jitter, which should be averaged out of the recovered carrier. For clarity, Figure 4.1 shows a loop model with these variables marked. The transfer function $\frac{\theta_s(s)}{\theta_I(s)}$ is obtained, as follows:

$$\theta_s(s) = \theta_o(s) - \theta_e(s)$$

$$= (H_b(s)-1)\ \theta_e(s)$$

$$\frac{\theta_s(s)}{\theta_I(s)} = \frac{-\tau s\ H_b(s)}{1 + k_v \tau H_b(s)\ F(s)}$$

$$= \frac{-\tau s\ (\tau_f s+1)\ \omega_n^2}{(1 + K_v\tau)\ (s^2 + 2\delta\omega_n s + \omega_n^2)} \qquad (4.3.1)$$

Other transfer functions of interest are the input-to-output transfer functions, $\frac{\theta_r(s)}{\theta_I(s))}$ or $\frac{\theta_o(s)}{\theta_I(s)}$, depending on which way the FLL is applied, (See Figure 2.1 and 2.2) and also, the loop phase transfer function $\frac{\theta_v(s)}{\theta_I(s)}$:

$$\frac{\theta_o(s)}{\theta_I(s)} = \frac{\theta_e(s)\ H_b(s)}{\theta_I(s)} = \frac{H_b(s)}{1 + K_v\tau\ H_b(s)\ F(s)} \qquad (4.3.2)$$

* Carrier Recovery (CR)

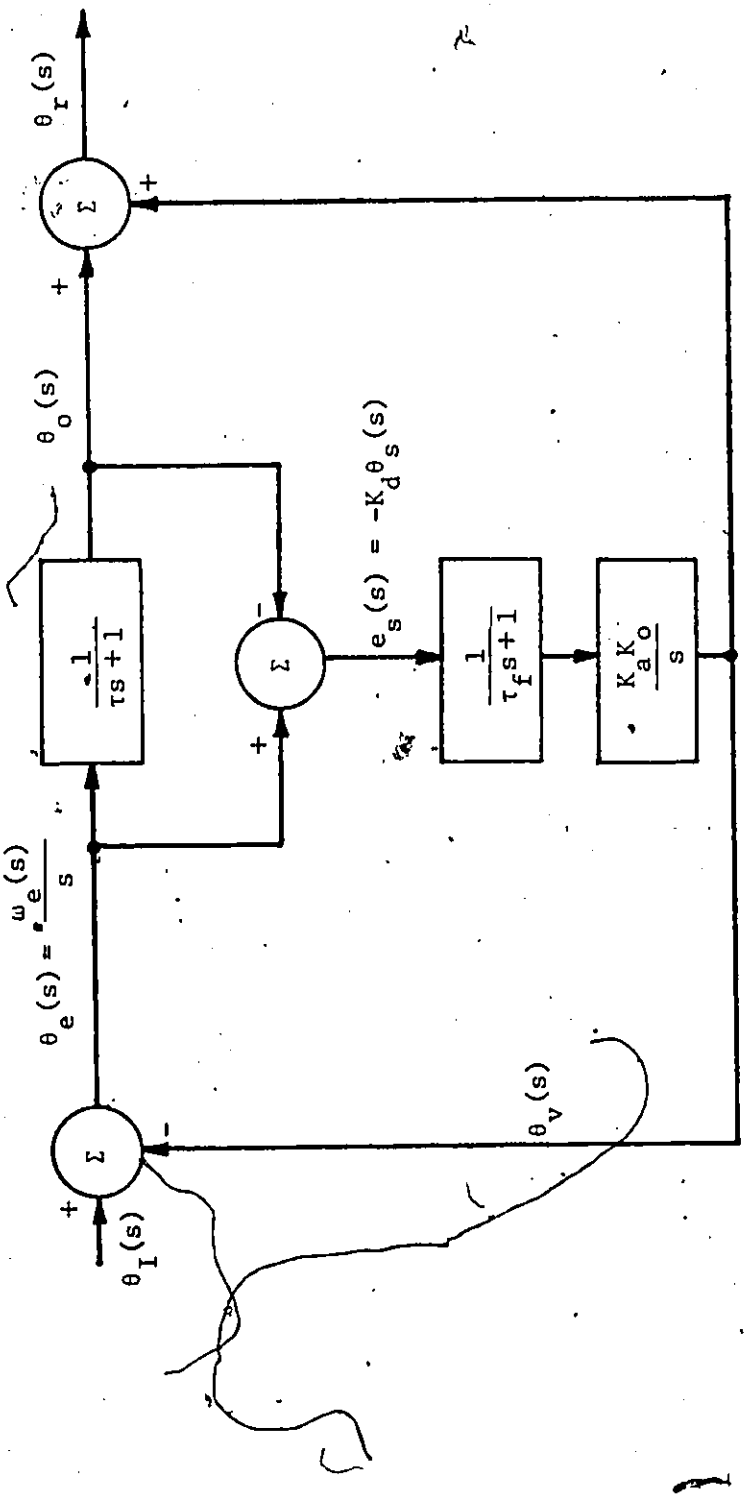

Figure 4.1: Linear Loop Model with Laplace Phase Variables Shown

$$\frac{\theta_r(s)}{\theta_I(s)} = \frac{\theta_s(s)}{\theta_I(s)} + 1$$

$$= 1 - \frac{\tau s\, H_b(s)}{1 + K_v \tau\, F(s)\, H_b(s)} \qquad (4.3.3)$$

and

$$\frac{\theta_v(s)}{\theta_I(s)} = \frac{k_v \tau\, F(s)\, H_b(s)}{1 + k_v \tau\, F(s)\, H_b(s)}$$

$$= \frac{k_v \tau\, \omega_n^2}{(1 + k_v \tau)\,(\delta^2 + 2\delta\omega_n s + \omega_n^2)} \qquad (4.3.4)$$

The Bode plots of these transfer functions are given in Figures 4.2 and 4.3 for the values as follows:

$$\tau_c = \tau = 10^{-6}$$

$$\tau_f = 10^3$$

$$K_v = 10^9$$

These values imply that:

$$\delta = \frac{1}{2}$$

$$\omega_n = 10^6$$

The significance of the transfer function will be appreciated where frequency "clicks" and threshold operation is discussed in the next section.

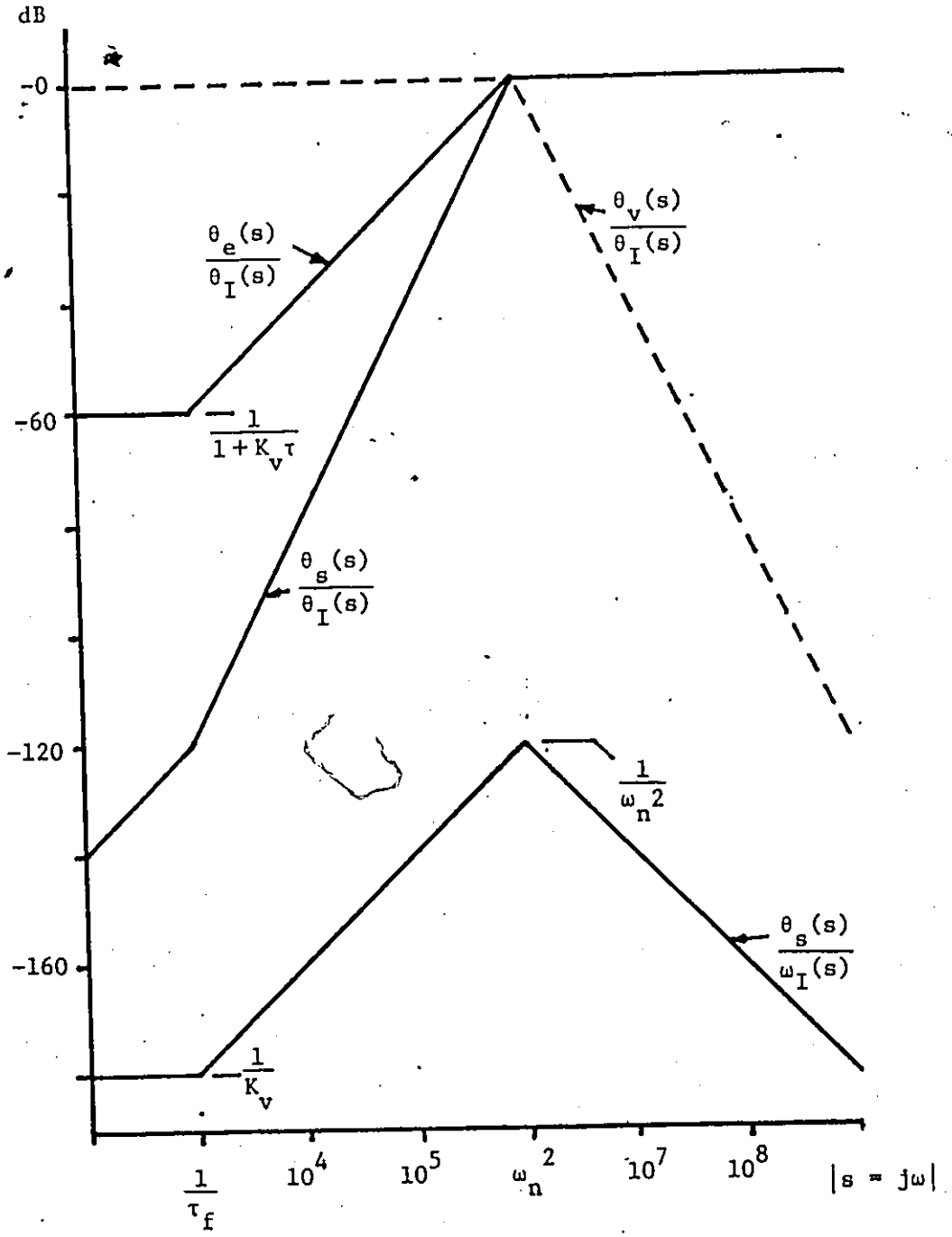

Figure 4.2: Bode Plots of Various Transfer Functions

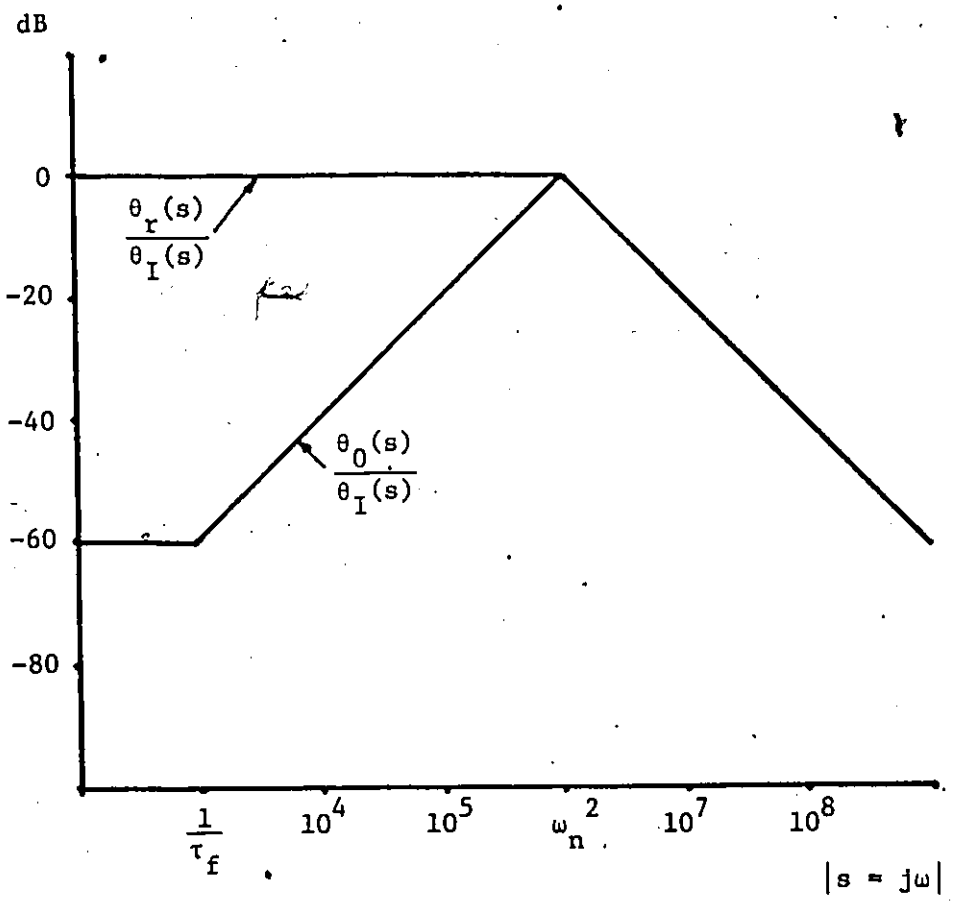

Figure 4.3: Bode Plots of Various Transfer Functions

4.4 Threshold Operation of the FLL

With the FLL being used as a carrier recovery circuit and since it is established that the FLL is a special application of an FMFB demodulator, it is important to consider the effect of frequency "clicks". See reference [5] or [18], for more details. A frequency "click" can be explained by considering the following expression for signal plus narrow band noise at a limiter-discriminator input.

$$v_i(t) = A\{1 + n_c(t)) \cos \phi(t) - n_s(t) \sin \phi(t)\} \qquad (4.4.1)$$

$$\text{where} \quad \phi(t) = \omega_o t + \int \omega_e(t)\, dt$$

A frequency "click" occurs when there is one zero crossing in $n_s(t)$ during a time period when $1 + n_c(t)$ is negative. It appears to the demodulator as though one extra or one less cycle of the carrier was present. When the rate of occurrence of cycle slips begins to significantly affect the SNR the demodulator is said to be at threshold. This phenomenon is similar in its effect to cycle slips in PLL's. What will happen when a frequency "click" occurs is that the recovered carrier will have a 2π radians transition in phase which probably will cause data detection errors during the transition. Obviously, the FLL should be designed to avoid frequency "clicks" if at all possible.

The FMFB demodulator is a threshold reduction FM demodulator. It works by the fact that a reduced signal frequency deviation allows a reduced bandwidth filter before demodulation. This allows the noise components $n_c(t)$ and $n_s(t)$ to be reduced and thereby reduce the probability of a "click" occurring. In FMFB design, this is referred to as the open-

loop threshold [16] since it is due to the limiter-discriminator in the open-loop response. Also in FMFB there is a feedback threshold which can occur even when the limiter-discriminator (LD) is operating above (open loop) threshold. The feedback threshold is caused by [8] intermodulation of the VCO phase noise and the FMFB demodulator input in-phase noise which produces an excess LD input phase noise in addition to the phase noise given by the difference of the FMFB demodulator input phase noise and the VCO phase noise. When this excess noise becomes significant compared to the difference between the input phase noise and VCO phase noise, then the FMFB demodulator is at the frequency threshold. To ensure threshold reduction, it is required to consider the combined effects of the open-loop and feedback thresholds [8,16].

Before proceeding any further with consideration of threshold, one slight difference between the FLL design considered so far and the FMFB design of reference [16] is the location of the STT in the loop. As part of the frequency detector (after limiter) it may not give the same open-loop threshold improvement as an equivalent STT could before the limiter since the limiter could tend to "harden" or emphasize any "clicks" so that a post-limiter STT would not be as effective. One easy solution to this problem would be to place another STT before the limiter and place a zero in the baseband part of the FLL for stability compensation. With a zero at the same frequency as the STT equivalent baseband pole, the loop dynamics would be unchanged. This alternate FLL is shown in Figure 4.4.

Rather than dealing with baseband SNR's in the application of

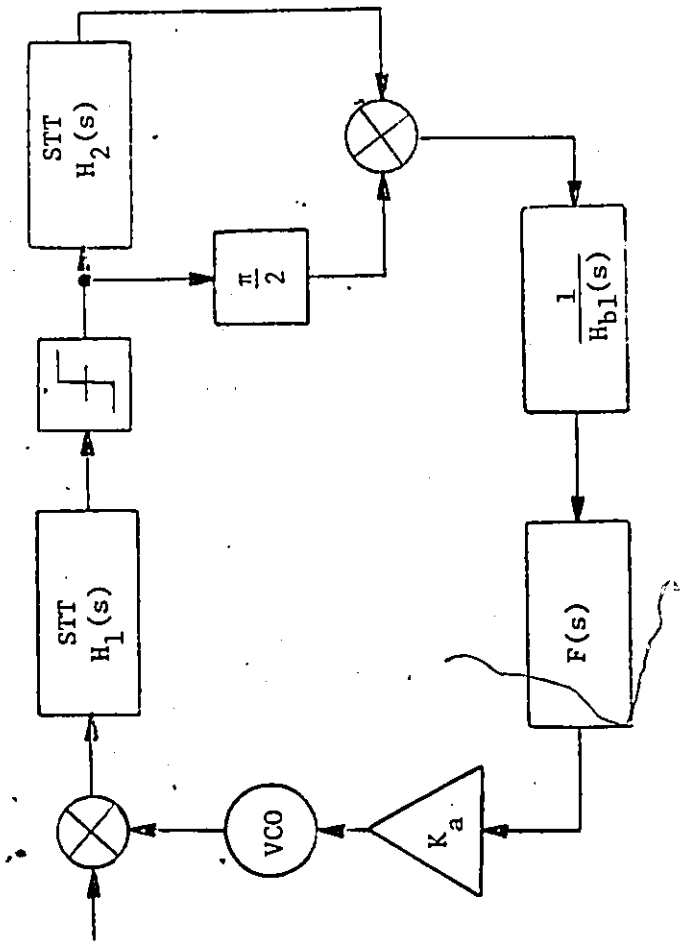

Figure 4.4: Block Diagram of FLL Modified to Reduce SNR Loss of Limiter

FLL's to carrier recovery, it makes more sense to use the probability of frequency "clicks" occurring or average "click" rate, etc. as the threshold parameter since the "click" rate can be translated into a BER due to threshold. In the case of the FLL open-loop threshold, this is given in reference [5] and was originally derived in reference [18] by Rice as:

$$N = \frac{\operatorname{erfc}(\sqrt{CNR})}{2\pi\tau\sqrt{3}} = \frac{\operatorname{erfc}\left(\sqrt{\frac{\tau A^2 \pi}{2N_o}}\right)}{2\pi\tau\sqrt{3}} \qquad (4.4.2)$$

where N is the "click" rate

$\frac{2}{\tau}$ is the STT 3 dB bandwidth

erfc(·) is the complementary error function

CNR is the carrier-to-noise ratio at the LD input

N_o is the input noise spectral density

Unfortunately, in the case of feedback threshold, there is no relationship available which describes the threshold in terms of clicks or any other discrete event, although it may be possible to derive the effect of excess phase noise associated with feedback threshold on the probability of error at detection. Presently, the only way to ensure that the excess phase noise associated with the feedback threshold will be insignificant compared to the phase noise predicted by the linear loop model is to design the FLL according to Enloe's [8,16] feedback threshold criterion:

$$\overline{\theta_{vn}^2}(t) \leq \frac{1}{9.6} \qquad (4.4.3)$$

where $\overline{\theta_{vn}^2}(t)$ is the mean square VCO phase noise due to loop input phase noise

The mean square VCO jitter is given by [16]:

$$\overline{\theta_{vn}^2(t)} = \frac{2N_o B_N}{A^2} \left| \frac{\theta_v(s=0)}{\theta_I(s=0)} \right|^2 \qquad (4.4.4)$$

where B_N is the loop noise bandwidth and from section 4.3 is given by:

$$B_N = \frac{\int_o^\infty \left| \frac{\theta_v(j\omega)}{\theta_I(j\omega)} \right|^2 df}{\left| \frac{\theta_v(0)}{\theta_I(0)} \right|^2} \qquad (4.4.5)$$

$$\simeq \frac{\omega_n}{2} = \frac{1}{2\tau} \text{ (Hertz)}$$

The mean square VCO phase noise jitter is then:

$$\overline{\theta_{vn}^2(t)} = \frac{N_o}{A^2 \tau} \qquad (4.4.6)$$

If it is assumed that the worst case (at which the CR circuit must work) CNR at the matched filter output is ρ_m, then:

$$\frac{\pi A^2 \tau_x}{2N_o} = \rho_m \qquad (4.4.7)$$

where $\frac{1}{\pi\tau_x}$ is the noise bandwidth of an IF matched (to data) in Hertz.

then:

$$\overline{\theta_{vn}^2} = \frac{\pi\tau_x}{2\rho_{m\tau}} \tag{4.4.8}$$

$$N = \frac{\operatorname{erfc}\left(\sqrt{\frac{\rho_m\tau}{\tau_x}}\right)}{2\pi\tau\sqrt{3}} < \frac{\exp\left(-\frac{\rho_m\tau}{\tau_x}\right)}{2\pi\tau\sqrt{3}} \tag{4.4.9}$$

For $\frac{\rho_m\tau}{\tau_x} = 20$, the average click rate is ≈ 1.5 clicks/hour and the mean square VCO phase noise is $\frac{\pi}{40}$ and both threshold effects do not seem to be a problem altough it is not known how the mean square VCO phase noise translates into a "click" rate.

This section which deals with the threshold performance could be refined and has not been tested by experiment. However, the relationships for threshold performance examined in this section are those needed to trade off the loop acquisition speed and tracking ability against noise performance of the loop, since any increase in τ improves noise performance, but reduces acquisition and tracking performance.

CHAPTER 5

CONCLUSIONS AND SUGGESTIONS FOR FURTHER WORK

5.1 Transient Analysis

5.1.1 The exact transient analysis has been done on several circuit models for a second order frequency tracking loop. As a result of the transient analysis, a number of conclusions can be drawn:

a) Fast reliable carrier acquisition can be achieved in 2 to 10 STT time constants τ from zero or non-zero state.

b) A second-order linear model is useful for estimating acquisition time, formulating a design procedure, and for analysis of high CNR noise if a hard limiter is used, and phase jitter.

c) The parameter $\tau_c = \frac{\tau_f}{1+K_v\tau}$ should be kept between τ and 4τ for good acquisition performance.

d) Limiters before the STT do not affect acquisition performance.

5.1.2 By allowing a non-linear degradation factor, b, to account for the slower responses due to non-linear effects at large initial frequency, offsets and non-zero state starting and after following the design procedure of Section 5.3.1 an empirical upper bound can be written using equation (3.6.2) as:

$$t_{a\omega} < 2b\tau \ln\left(\frac{\tau\omega_{IM}}{\theta_{sm}}\right) \qquad \omega_{IM} < \frac{1}{\tau} \tag{5.1.1}$$

where the value for b is approximately two.

5.2 Noise Considerations

5.2.1 A hard limiter should be used before the STT, as shown in Figure 5.1 in order to stop amplitude variations and amplitude noise on the carrier causing phase jitter.

5.2.2 Since the FLL is equivalent to an FMFB demodulator, previous analysis done on FMFB demodulators is useful in considering the low CNR case for Gaussian noise.

5.2.3 Gaussian noise can cause frequency "clicks" at low CNR's which will probably cause symbol detection errors in the demodulator, however, by restricting the STT noise bandwidth and the noise bandwidth of the loop which are both proportional to $\frac{1}{\tau}$ for the design procedure recommended, the threshold effects can be made insignificant.

5.2.4 It appears in the consideration of the noise versus acquisition time tradeoff that acquisition could be achieved in between 10 and 100 times the symbol period for 2 bits/symbol modulations with completely insignificant effects due to frequency "clicks" if a hard limiter is used, although more work and experimental results are required to verify this.

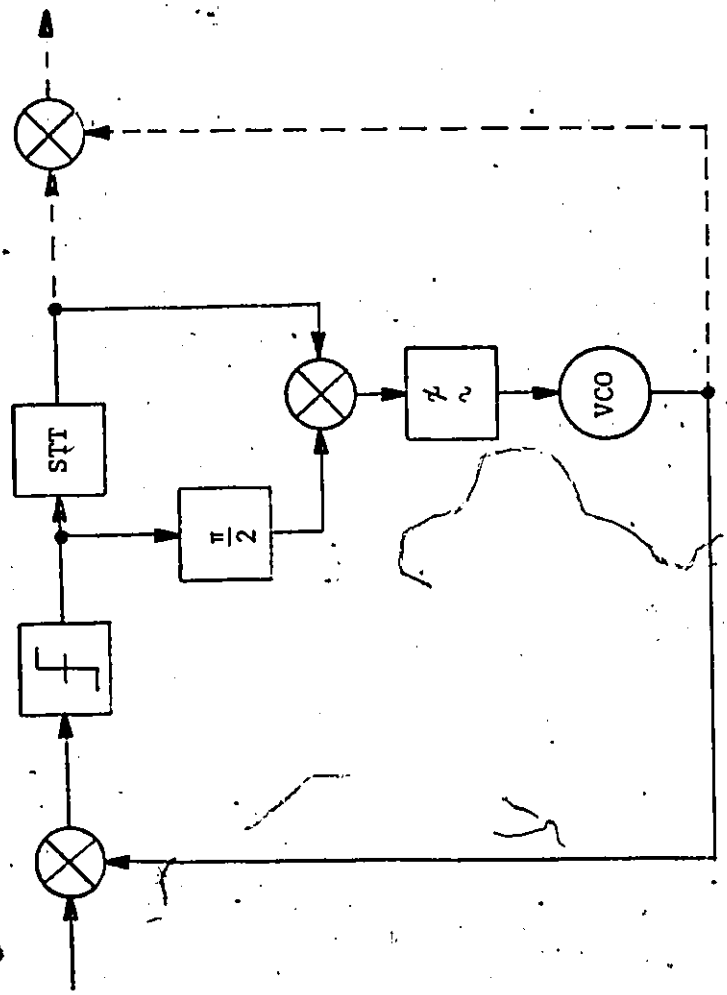

Figure 5.1: Block Diagram of Recommended FLL

5.3 Design Procedure

5.3.1 In order to achieve a good design, the following design procedure may be followed:

a) Choose τ, trading off noise performance and acquisition performance using equations (4.4.7), (4.4.8) and (3.6.2).

b) Choose K_v according to inequality (3.6.3).

c) Choose τ_f according to (3.6.4).

5.3.2 It should be noted that after following this procedure, nothing can reduce acquisition time (assuming θ_{SM} and ω_{IM} and circuit model remain unchanged) except reducing τ and repeating 5.3.1 (b) and (c) over again.

5.4 Suggestions for Further Work

5.4.1 Investigate the bias problem encountered for $\tau_c = \tau/10$ in the bandpass differential equation models for acquisition performance.

5.4.2 Further investigate the feedback threshold effect and the Enloe feedback threshold criterion and attempt to relate it to bit error rate performance.

5.4.3 Block diagrams shown in Figures 5.2 and 5.3 may give better acquisition performance and noise performance.

In Figure 5.2, the STT with transfer function $H_1(s)$ reduces the SNR loss [9] due to the first limiter. The equalizer with transfer

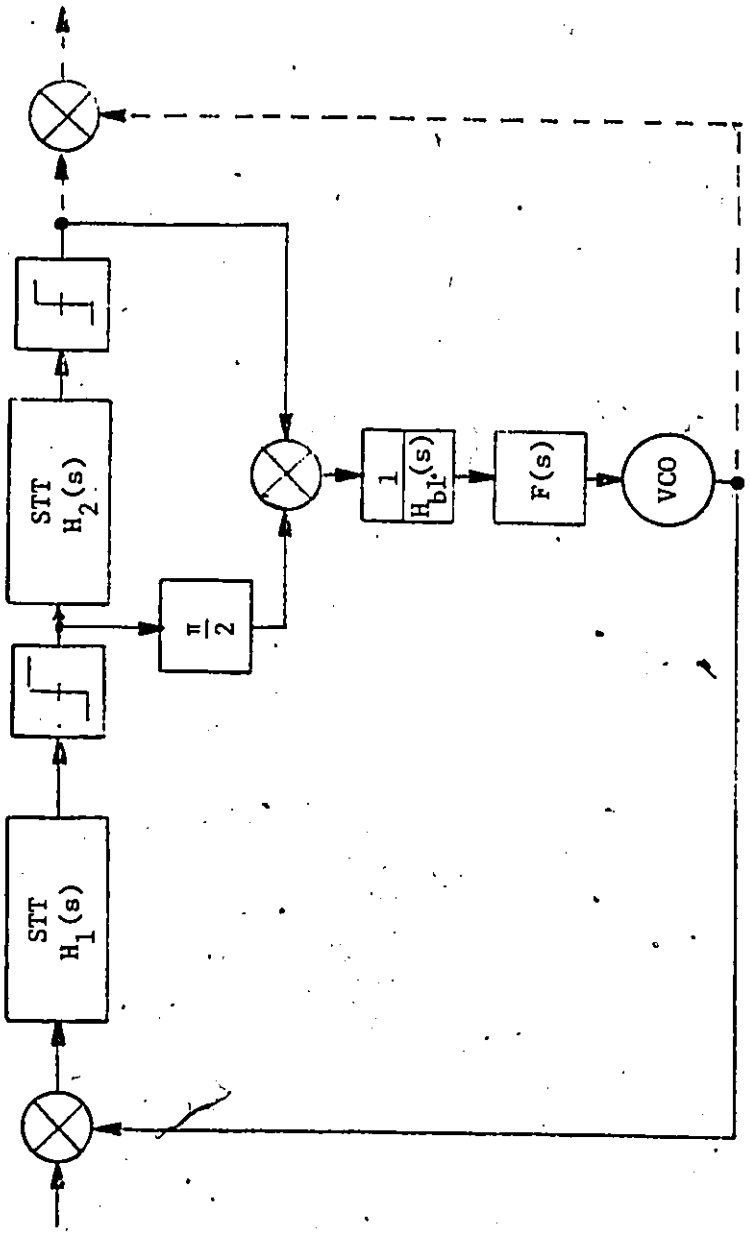

Figure 5.2: Block Diagram of FLL which may Provide Improved Noise and Acquisition Performance

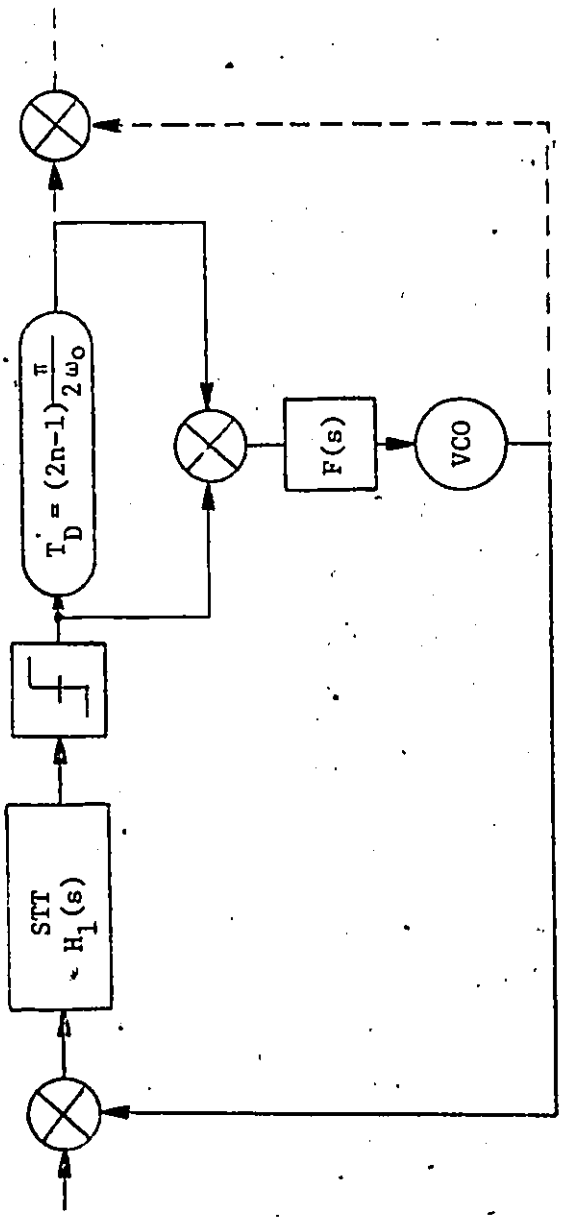

Figure 5.3: Block Diagram of FLL with Linear Frequency Detector (n an integer)

function $1/H_{bl}(s)$ where $H_{bl}(s)$ is the baseband equivalent of $H_1(s)$, is sufficient to ensure stability. The second limiter is intended to reduce acquisition time and noise degradation. The second limiter also makes the steady-state error signal a monotonically increasing function of frequency. In Figure 5.3, the frequency detector shown in the loop is linear over frequency range $2\omega_o/(2n-1)$ with sensitivity of $B^2\pi(2n-1)/(2\omega_o)$. Otherwise, it is expected that the block diagram of Figure 5.3 would behave similarly to that of Figure 5.1.

5.4.4 Refine the estimate of acquisition time in terms of data symbol time period with noise effects on bit error rate as a restriction.

5.4.5 A comparison study of the PLL with the FLL would be useful.

APPENDIX A

DERIVATION OF STEADY STATE ERROR SIGNAL IN PRESENCE OF GAUSSIAN NOISE (NO LIMITER)

The STT input signal is:

$$v_i(t) = (A + n_c(t))\cos \omega_f t - n_s(t) \sin \omega_f t$$

The error signal may be written as:

$$e_s'(t) = v_p(t) \int_0^t h(\alpha)\, v_i(t-\alpha)\, d\alpha$$

where

$$h(t) = \frac{2}{\tau} e^{\frac{-t}{\tau}} u(t) (\cos \omega_d t - \frac{1}{\tau\omega_d} \sin \omega_d t)$$

$$v_p(t) = -(A + n_c(t)) \sin \omega_f t - n_s(t) \cos \omega_f t$$

When $v_p(t)$ and $v_i(t-\alpha)$ are multiplied together, the sum and difference frequency components arise. By neglecting the sum frequency components, then the difference frequency error signal may be written as:

$$e_s(t) = -\frac{1}{2} \int_0^t h(\alpha)\, (n_c(t)+A)\, (n_c(t-\alpha)+A) \sin \omega_f\alpha\, d\alpha$$

$$+\frac{1}{2} \int_0^t h(\alpha)\, (n_c(t)+A)\, (n_s(t-\alpha)) \cos \omega_f\alpha\, d\alpha$$

$$-\frac{1}{2} \int_0^t h(\alpha)\, n_s(t)\, (n_c(t-\alpha)+A) \cos \omega_f\alpha\, d\alpha$$

$$-\frac{1}{2} \int_0^t h(\alpha)\, n_s(t)\, n_s(t-\alpha) \sin \omega_f\alpha\, d\alpha$$

By taking the limit as $t \to \infty$ of $e_s(t)$ and taking the expectation, then,

$$e_{ss} = E\{\lim_{t\to\infty} e_s(t)\} = -\frac{1}{2}\int_0^\infty h(\alpha)\,(A^2 + 2R_n(\alpha))\,\sin\omega_f\alpha\,d\alpha$$

$$= -\frac{1}{\tau}\int_{-\infty}^{\infty} (A^2 + 2R_n(\alpha))\,e^{-\frac{\alpha}{\tau}}\left(\cos\omega_d\alpha\,\sin\omega_f d - \frac{1}{\tau\omega_d}\sin\omega_d\alpha\,\sin\omega_f\alpha\right)d\alpha$$

where $R_n(\alpha)$ is the autocorrelation of the input noise. It is assumed that the input noise has a correlation time, τ_x, and,

$$R_n(\alpha) = \frac{N_o}{2\tau_x}\,e^{-\frac{|\alpha|}{\tau_x}}$$

Now by expanding the sinusoidal terms:

$$e_{ss} = -\frac{1}{2\tau}\int_o^\infty (A^2 + 2R_n(\alpha))e^{-\frac{\alpha}{\tau}}\left(\sin(\omega_d+\omega_f)\alpha - \sin(\omega_d-\omega_f)\alpha\right.$$

$$\left. -\frac{1}{\tau\omega_d}\cos(\omega_d-\omega_f)\alpha + \frac{1}{\tau\omega_d}\cos(\omega_d+\omega_f)\alpha\right)d\alpha$$

The signal component e_{sss} ($2R_n(\alpha)$ left out) is:

$$e_{sss} = -\frac{A^2}{2\tau}\left[\frac{\omega_d+\omega_f}{\frac{1}{\tau^2}+(\omega_d+\omega_f)^2} - \frac{\omega_d-\omega_f}{\frac{1}{\tau^2}+(\omega_d-\omega_f)^2}\right.$$

$$\left. - \frac{\frac{1}{\tau^2\,\omega_d}}{\frac{1}{\tau^2}+(\omega_d-\omega_f)^2} + \frac{\frac{1}{\tau^2\,\omega_d}}{\frac{1}{\tau^2}+(\omega_d+\omega_f)^2}\right]$$

$$= -\frac{A^2}{2}\left[\frac{\tau\left(\omega_d+\omega_f+\frac{1}{\tau 2\,\omega_d}\right)}{1+\tau^2\,(\omega_d+\omega_f)^2} - \frac{\tau\left(\omega_d-\omega_f+\frac{1}{\tau 2\,\omega_d}\right)}{1+\tau^2\,(\omega_d-\omega_f)^2}\right]$$

The expression may be simplified by substituting for ω_d and ω_f

$$\omega_d = \omega_o\sqrt{1-\frac{1}{4Q^2}}$$

$$\omega_f = \omega_o + \omega_e$$

$$\frac{1}{\tau^2\omega_d} = \frac{1}{\tau\sqrt{4Q^2-1}}$$

$$\tau\left(\omega_d+\omega_f+\frac{1}{\tau^2\omega_d}\right) = \sqrt{4Q^2-1} + 2Q + \tau\omega_e + \sqrt{4Q^2-1}$$

$$= \frac{4Q^2}{\sqrt{4Q^2-1}} + 2Q + \tau\omega_e$$

$$\tau\left(\omega_d-\omega_f+\frac{1}{\tau^2\omega_d}\right) = \frac{4Q^2}{\sqrt{4Q^2-1}} - 2Q - \tau\omega_e$$

$$\approx \frac{1}{4Q} - \tau\omega_e \qquad Q >> 1$$

$$\tau^2\,(\omega_d-\omega_f)^2 = \left(\sqrt{4Q^2-1} - 2Q - \tau\omega_e\right)^2$$

$$\approx \left(-\frac{1}{4Q} - \tau\omega_e\right)^2 \qquad Q >> 1$$

$$\tau^2\,(\omega_d+\omega_f)^2 = \left(\sqrt{4Q^2-1} + 2Q + \tau\omega_e\right)^2$$

For $Q >> 1$ and $\tau\omega_e << 2Q$, then:

$$e_{sss} \simeq -\frac{A^2}{2}\left[\frac{1}{2Q} - \frac{\frac{1}{4Q} - \tau\omega_e}{1 + \tau^2\,\omega_e^2}\right]$$

$$\text{Since } \frac{4Q^2}{\sqrt{4Q^2 - 1}} \simeq 2Q \simeq \frac{1}{4Q} \quad Q >> 1$$

For $\tau\omega_e << 1$:

$$e_{sss} \simeq -\frac{A^2}{2}\left[-\frac{1}{2Q} + \tau\omega_e\right]$$

$$= -\frac{A^2}{2}\left[-\frac{1}{2Q} + \frac{2Q}{\omega_o}\,\omega_e\right]$$

The noise component of the expected steady-state error signal has the same form as the signal component except that the quantity

$$A^2\, e^{-\frac{\alpha}{\tau}}$$

is replaced by the quantity:

$$R_n(\alpha)\, e^{-\frac{\alpha}{\tau}} = \frac{N_o}{2\tau_x}\, e^{-\frac{|\alpha|}{\tau_x}}\, e^{-\frac{\alpha}{\tau}}$$

and since $\alpha > 0$

then $$R_n(\alpha)\, e^{-\frac{\alpha}{\tau}} = \frac{N_o}{2_x}\, e^{-\frac{\alpha}{\tau+\tau_x}}$$

Therefore, the noise component of the expected steady-state value of the difference frequency error signal is:

$$e_{ssn} = \frac{N_o}{2\tau_x}\left[-\frac{1}{2Q} + \tau\omega_e\right] \qquad \begin{array}{l} Q \gg 1 \\ \tau\omega_e \ll 1 \\ \tau \gg \tau_x \end{array}$$

and

$$e_{ss} = -\frac{1}{2Q} + \tau\omega_e \quad \left(\frac{N_o}{2\tau_x} + \frac{A^2}{2}\right)$$

REFERENCES

[1] Asahara, M., Toyonoga, N., Sasaki, S., Miyo, T., "Analysis of carrier recovery adopting a narrow band pass filter with AFC loop", Proc. of Third Int'l. Conference on Digital Satellite Communications, Kyoto, Japan, November 11-13, 1975, pp. 99-104.

[2] Nuspl, P. P., Lyons, R. G., Bedford, R., "Slim TDMA project", Proc. of Fifth Int'l. Conference on Digital Satellite Communication, Genoa, Italy, March 23-26, 1981, pp. 353-360.

[3] Bedford, R., "Design of a programmable TDMA terminal", NTC 80, Houston, pp. 71.3.1-8.

[4] Taub, H., Schlling, D. L., Principles of Communication Systems, McGraw Hill, New York, 1971, Ch. 9 and Ch. 10.

[5] Haykin, S., Communication Systems, John Wiley and Sons, New York, 1978, pp. 131-132, Ch. 1, 2, 4, 5.

[6] Desoer, C. A., Kuh, E. S., Basic Circuit Theory, McGraw Hill, New York, 1969, pp. 310-317, 542-543.

[7] Chaffee, J. G., "The application of negative feedback to frequency modulation systems", Proc. IRE 27, May 1939, pp. 317-331.

[8] Enloe, L. H., "Decreasing the threshold in FM by frequency feedback", Proc. IRE 50, January 1962, pp. 18-30.

[9] Gardner, F. M., Phaselock Techniques (2nd Edition), John Wiley and Sons, New York, 1979, Ch. 5, 6, 9.

[10] Gardner, F. M., "Hangup in phase-lock loops", IEEE Trans., COM-25, Oct. 1977, pp. 1210-1214.

[11] Gardner, F. M., "Comparison of QPSK carrier regenerator circuits for TDMA application", ICC 74, Minneapolis, June 17-19, 1974, pp. 43B-1 to 43B-5.

[12] Mariuz, S., "The limit switched loop: An improved carrier recovery algorithm for burst mode operation", Communication Research Lab., McMaster University, Hamilton, Canada, Report No. CRL-47, June 1977.

[13] Tang, S. K., "Second-order limit-switched loop", Communication Research Lab., McMaster University, Hamilton, Canada, Report No. CRL-70, January 1980.

[14] Asahara, M., Toyonoga, Sasaki, S., Miyo, T., "A 4-phase PSK MODEM for SCPC satellite communication system", ICC 75, San Francisco, 16-18, June 1975, pp. 12.28-12.32.

[15] Yokoyama, S., Kato, K., Noguchi, T., Kusama, N., Otani, S., "The design of a PSK modem for the Telesat TDMA system", ICC 75, San Francisco, June 16-18, 1975, pp. 44.11-44.15.

[16] Klapper, J., Frankle, J. T., Phase-Locked and Frequency Feedback Systems, Academic Press, New York and London, 1972, Ch. 3, 4, 7.

[17] Private communication (photograph) from "R. Bedford, F. Vaughan, R. G. Lyons", Miller Communication Systems Limited, Kanata, Ontario, Canada, January 1980.

[18] Rice, S. O., "Noise in FM Receivers", Symposium Proceedings of Time Series Analysis, edited by M. Rosenblatt, John Wiley and Sons, New York, 1963, pp. 395-422.

[19] Carson, J. R., "Frequency modulation: Theory of feedback receiving circuit", BSTJ, Vol. 18, No. 3, July 1939, pp. 395-403.